A&A 505, 441–462 (2009)
DOI: 10.1051/0004-6361/200912531

Astronomy & Astrophysics

High-resolution UVES/VLT spectra of white dwarfs observed for the ESO SN Ia Progenitor Survey

III. DA white dwarfs⋆

D. Koester[1], B. Voss[2,1], R. Napiwotzki[3], N. Christlieb[4], D. Homeier[5], T. Lisker[6,8], D. Reimers[7], and U. Heber[8]

[1] Institut für Theoretische Physik und Astrophysik, Universität Kiel, 24098 Kiel, Germany
e-mail: koester@astrophysik.uni-kiel.de
[2] Zeiss-Planetarium, LWL-Museum für Naturkunde, 48161 Münster, Germany
[3] Centre for Astrophysics Research, University of Hertfordshire, College Lane, Hatfield AL10 9AB, UK
[4] Landessternwarte, Zentrum für Astronomie der Universität Heidelberg, Königstuhl 12, 69117 Heidelberg, Germany
[5] Institut für Astrophysik, Georg-August-Universität, Friedrich-Hund-Platz 1, 37077 Göttingen, Germany
[6] Astronomisches Rechen-Institut, Zentrum für Astronomie der Universität Heidelberg, Mönchhofstr. 12–14, 69120 Heidelberg, Germany
[7] Hamburger Sternwarte, Gojenbergsweg 112, 21029 Hamburg, Germany
[8] Dr. Karl Remeis Observatory, University of Erlangen-Nürnberg, Sternwartstr. 7, 96049 Bamberg, Germany

Received 19 May 2009 / Accepted 24 July 2009

ABSTRACT

Context. The ESO Supernova Ia Progenitor Survey (SPY) took high-resolution spectra of more than 1000 white dwarfs and pre-white dwarfs. About two thirds of the stars observed are hydrogen-dominated DA white dwarfs. Here we present a catalog and detailed spectroscopic analysis of the DA stars in the SPY.
Aims. Atmospheric parameters effective temperature and surface gravity are determined for normal DAs. Double-degenerate binaries, DAs with magnetic fields or dM companions, are classified and discussed.
Methods. The spectra are compared with theoretical model atmospheres using a χ^2 fitting technique.
Results. Our final sample contains 615 DAs, which show only hydrogen features in their spectra, although some are double-degenerate binaries. 187 are new detections or classifications. We also find 10 magnetic DAs (4 new) and 46 DA+dM pairs (10 new).

Key words. stars: white dwarfs

1. Introduction

The ESO SN Ia Progenitor Survey (SPY) is a radial velocity survey that was conducted to test the double-degenerate channel of the formation of supernovae Ia. About 800 white dwarfs were observed (most of them twice) in the course of the survey, assembling a large collection of high quality white dwarf spectra. Most of the targets for the SPY were selected from the White Dwarf catalog (McCook & Sion 1999), MCS further on, from the Hamburg/ESO Survey (Wisotzki et al. 1996; Christlieb et al. 2001), HES further on, and from the Hamburg Quasar Survey (Hagen et al. 1995), HQS further on. Some additional objects come from the Montreal-Cambridge survey (Demers et al. 1990; Lamontagne et al. 2000) and from the Edinburgh-Cape survey (Kilkenny et al. 1991). A detailed discussion of the target selection is given in Napiwotzki et al. (2001, 2003). While some of the input catalogs, e.g. HES and HQS, have fairly well understood selection criteria, for the combined input catalog this would be very difficult, since the only criteria used were "spectroscopic identification (at least from objective prism spectra) and $B < 16.5$" (Napiwotzki et al. 2001).

The high quality spectra of white dwarfs were employed for a number of studies beyond the original scope of the SPY, the search for double-degenerate binaries. Koester et al. (2001) derived temperatures and gravities from a preliminary sample of about 200 objects; 71 helium-rich stars of spectral type DB and DBA were studied in Voss et al. (2007), and approximately 60 objects with detected Ca II resonance lines were discussed in Koester et al. (2005). Pauli et al. (2003, 2006) studied the 3D kinematics using the SPY data, new DO and PG1159 stars have been identified by Werner et al. (2004). The hot subdwarf population has been studied by Lisker et al. (2005) and Stroeer et al. (2007).

The number of newly detected white dwarfs is of course dwarfed by the results from the Sloan Digital Sky Survey (e.g. Kleinman et al. 2004; Eisenstein et al. 2006). It is also possible to extract samples with much better controlled and understood selection effects from the SDSS data base. Thus, we will not produce yet another white dwarf mass distribution or luminosity function here. However, our sample contains much brighter objects than the typical SDSS white dwarf. These objects, and in particular the magnetic stars, binaries, or new variables will be much easier to study in follow-up observations than the faint SDSS objects. Moreover, the white dwarf parameters presented here are an important ingredient of the kinematic studies mentioned above and the analysis and interpretation of the binary results, starting with the simple distinction between helium core and carbon/oxygen core white dwarfs.

⋆ Based on data obtained at the Paranal Observatory of the European Southern Observatory for programmes 165.H-0588 and 167.D-0407.

2. Observations

Since several of the papers above have given a detailed description of the data properties and further references, we only briefly summarize this information here.

The spectra were obtained with UVES, a high resolution echelle spectrograph at the ESO VLT telescope. UVES was used in a dichroic mode, resulting in small gaps, ≈80 Å wide, at 4580 Å and 5640 Å in the final merged spectrum. The spectral resolution at Hα is $R = 18\,500$ or better, and the S/N per binned pixel (0.05 Å) is $S/N = 15$ or higher. The total wavelength range covered is ≈3500 to 6650 Å.

The spectra were reduced with the ESO pipeline for UVES, including the merging of the echelle orders and the wavelength calibration. Koester et al. (2001) found that the quality of these automatically extracted spectra was very good, except for a quasi-periodic wave-like pattern that occurs in some of the spectra. The reduction has since been further improved by additional processing by collaborators of the SPY at the University of Erlangen-Nürnberg. The most important step was utilizing the featureless spectra of DC white dwarfs to remove almost completely the large scale variations of the spectral response function (Napiwotzki et al. 2001, 2003). Some artifacts remain in the data, but they do not significantly affect the spectral analysis.

2.1. Model atmosphere fits

The spectral analysis of these data was originally performed by Voss (2006). Since then, the models were significantly improved by including in a consistent way the Balmer line broadening due to simultaneous interactions with neutral and charged perturbers. An up-to-date description of the methods and input physics is presented in Koester (2009). We have therefore repeated the whole fitting process for all objects; the major differences to Voss (2006) appear, as expected, at the cool end of the DA sequence.

The χ^2 minimization fitting routine is based on the Levenberg-Marquardt algorithm (Press et al. 1992) to derive the best fitting effective temperature and surface gravity for each spectrum. Some more details on the fitting process can be found in Homeier et al. (1998). For the present study we applied pure hydrogen models and fitted the Balmer lines Hα to H9. To demonstrate the typical quality of the data and of the model fits, we present the results for the arbitrarily chosen entries 301 to 310 from Table 1. The header of each panel gives the name, effective temperature, and surface gravity of the fit. Shown are the six lowest Balmer lines.

3. Data and atmospheric parameters for DAs

Table 1 lists the results of the model fitting for 615 apparently normal DA white dwarfs. Of those, 187 are newly identified DAs, 111 from the HES (Christlieb et al. 2001, designation HE) and 76 from the HQS (Homeier et al. 1998, designation HS) surveys. The primary designation of the objects in the first column is WD, if the objects appear in the SIMBAD or MCS databases and were known to be spectroscopically identified white dwarfs prior to the start of the SPY. A few objects have EC or MCT designations, if they were identified in the Edinburgh-Cape (Kilkenny et al. 1991) or Montreal-Cambridge-Tololo (Demers et al. 1990; Lamontagne et al. 2000) surveys, but don't seem to have WD designations. Column 5 gives a few alternative names. This list is not intended to be complete, but additional information can easily be found in SIMBAD or MCS.

For the remainder of the objects we use HE or HS designations, depending on the original catalog. In this case there are three different meanings of Col. 5

- if empty, there is no entry in either the SIMBAD or the MCS database and we assume that this is a new detection of the HQS or HES;
- if there is an entry in parentheses, this means that there is an entry in SIMBAD, but no spectroscopic identification as a white dwarf, at least not prior to identification in a publication related to HQS, HES, or SPY. This mostly concerns catalogs of blue or large proper motion objects. Some objects are also contained in more recent catalogs, e.g. Sloan Digital Sky Survey = SDSS (Adelman-McCarthy et al. 2008), or Two Micron All Sky Survey = 2MASS, (Cutri et al. 2003), but not identified as white dwarfs;
- if there is a regular entry in Col. 5, this describes a recent spectroscopic identification, which was unknown at the time of our target selection. Catalog entries here are SDSS (Kleinman et al. 2004; Eisenstein et al. 2006), BGK (Brown et al. 2006), Kawka06 (Kawka & Vennes 2006).

The magnitude column lists the V magnitude, if available from the SIMBAD or MCS databases. If the number is followed by a B, this is either a Johnson B magnitude, or, in most cases, a photographic magnitude from the MCT, HQS, or HES surveys. mc denotes a Greenstein multichannel magnitude, obtained from the MCS catalog. The errors of the photographic magnitudes are typically much larger (0.1−0.2 mag) than suggested by the two decimal places, which are kept only to obtain a more homogeneous table.

Since most stars have more than one spectrum observed, the parameters are the weighted averages of the individual solutions, with the inverse square of the formal 1σ uncertainties as weights. The 1σ final uncertainties given in Table 1 are obtained from the individual values and should only be used as an indicator of the quality of the data. As is well known, with spectra of the quality used here, the systematic errors from the reduction and fitting process are usually much larger than the purely statistical uncertainties. We estimated more realistic uncertainties by comparing the differences between solutions from several spectra of the same object. For 592 objects with multiple solutions we obtain standard deviations of $\sigma(T_{\rm eff}) \approx 2.5\%$ and $\sigma(\log g) \approx 0.09$. These should be regarded as lower limits, because the different spectra still used the same observational setup, theoretical models, and fitting procedures. The uncertainties are definitely larger than this at the high temperature end above 50 000 K, because NLTE effects are not considered in our models. They are also larger, in particular for the surface gravity, at temperatures below 8000 K, because the spectra become less sensitive to this parameter, and because the neutral broadening of the Balmer lines higher than Hγ is only approximative.

Another method to estimate the size of the uncertainties is the comparison of results by different authors for the same objects. The most interesting recent study is the work by Liebert et al. (2005) on the DA white dwarfs in the Palomar Green Survey. Eliminating DAs with $T_{\rm eff}$ below 8000 K or above 50 000 K (see above), as well as the double degenerates, leaves 85 objects in common. Figure 2 shows the comparison for the effective temperatures, and Fig. 3 for the surface gravities. The systematic shift in $T_{\rm eff}$ for the whole sample is 1.2%, with our temperatures being slightly higher. For $\log g$ the shift is 0.08, with our values lower. We can estimate the intrinsic uncertainties of our determinations by first correcting for these systematic shifts. Comparing the corrected parameters with those

Table 1. Fit results for hydrogen atmosphere stars.

Object	RA(2000)	Dec(2000)	mag(band)	Aliases	$T_{\rm eff}$ [K]	$\sigma(T_{\rm eff})$ [K]	$\log g$	$\sigma(\log g)$	Spectra	Remarks
WD 2359−324	00:02:32.36	−32:11:50.7	15.87 B	MCT 2359−3228	22 478	57	7.742	0.008	3	
WD 0000−186	00:03:11.21	−18:21:57.6	16.29 B	MCT 0000−1838, GD 575	15 264	43	7.846	0.009	2	
HS 0002+1635	00:04:43.34	+16:52:16.7	15.30 B	(PHL 647)	25 878	36	7.859	0.005	2	
WD 0005−163	00:07:34.80	−16:05:31.8	16.29 mc	G 158−132, GR 509	15 141	25	7.594	0.009	2	NOV(1)
					11 684	31	7.689	0.012	2	amb
WD 0011+000	00:13:39.19	+00:19:23.1	15.31	G 031−035, WOLF 1, SDSS	9472	7	8.037	0.010	2	
WD 0013−241	00:16:12.63	−23:50:06.4	15.36	MCT 0013−2406, GR 458	18 529	26	7.896	0.005	2	
WD 0016−258	00:18:44.49	−25:36:42.2	16.07 B	MCT 0016−2553	10 828	14	8.022	0.008	2	DAV
WD 0016−220	00:19:28.23	−21:49:04.9	15.31	GD 597, PHL 2856	13 264	51	7.779	0.006	2	
WD 0017+061	00:19:40.99	+06:24:06.2	14.55 B	PG 0017+061, PHL 790	28 149	35	7.749	0.006	2	
WD 0018−339	00:21:12.90	−33:42:27.4	14.70	GD 603, BPM 46232	20 626	24	7.842	0.005	2	
WD 0024−556	00:26:41.08	−55:24:44.9	15.21	L 170−27, BPM 16115	10 157	7	8.737	0.006	2	
WD 0027−636	00:29:56.79	−63:24:58.3	15.29 B	RE 0029−632, EUVE J0030−634	58 129	210	7.769	0.011	2	
WD 0028−474	00:30:47.16	−47:12:36.9	15.24 B	HE 0028−4729, JL 192	17 394	27	7.653	0.005	2	DDd
WD 0029−181	00:32:30.33	−17:53:23.3	16.05 B	HE 0029−1809,KUV 00300−1810	13 578	76	7.831	0.010	2	
HE 0031−5525	00:33:36.03	−55:08:37.5	15.94 B	(JL 197)	11 662	28	7.829	0.010	2	DAV
MCT 0031−3107	00:34:24.85	−30:51:25.6	16.43 B		40 698	236	7.777	0.023	2	
HE 0032−2744	00:34:37.91	−27:28:20.0	16.28 B		23 947	60	7.812	0.008	2	
WD 0032−317	00:34:49.82	−31:29:54.3	15.62 B	MCT 0032−3146	36 965	100	7.192	0.014	2	
WD 0032−175	00:35:17.47	−17:18:51.1	14.94 B	MCT 0032−1735, GR 511	9652	7	8.080	0.007	2	
WD 0032−177	00:35:25.20	−17:30:40.4	15.70	KUV 00329−1747	17 210	38	7.816	0.009	2	
WD 0033+016	00:35:35.93	+01:53:06.5	15.52	L 1011−71, G 001−007	10 669	11	8.789	0.006	2	NOV(2)
MCT 0033−3440	00:36:13.89	−34:23:35.7	16.42 B	HBQS 0033−3440	15 890	56	8.184	0.007	2	
WD 0037−006	00:40:22.94	−00:21:31.1	14.85	PG 0037−006, PB 6089, SDSS	16 403	19	7.738	0.004	3	DDd
HE 0043−0318	00:46:18.38	−03:02:00.8	15.48 B		14 086	33	7.732	0.004	2	
WD 0047−524	00:50:03.74	−52:08:17.1	14.20	BPM 16274, L 219−048	18 811	17	7.732	0.003	2	
HS 0047+1903	00:50:12.43	+19:19:49.3	15.50 B		17 135	25	7.823	0.005	3	
WD 0048−544	00:51:08.87	−54:11:21.2	15.29	HE 0048−5427, L 220−145	17 870	20	7.976	0.004	2	
WD 0048+202	00:51:11.00	+20:31:22.3	15.36	PG 0048+202	20 363	24	7.890	0.004	3	
HE 0049−0940	00:52:15.30	−09:24:20.3	16.00 B	(PHL 3044)	13 592	42	7.704	0.003	2	
WD 0050−332	00:53:17.43	−32:59:56.8	13.36	MCT 0050−3316, SB 360	35 570	21	7.874	0.003	3	
WD 0052−147	00:54:55.86	−14:26:09.1	15.12	MCT 0052−1442, GD 662	25 950	26	8.224	0.004	2	
WD 0053−117	00:55:50.33	−11:27:31.3	15.26	L 796−10, LP 706−065	6515	7	7.037	0.013	2	
WD 0101+048	01:03:50.01	+05:04:29.2	13.96	G 002−017, G 001−045	8387	5	7.992	0.007	2	DDs
WD 0102−185	01:04:53.10	−18:19:50.2	16.40	MCT 0102−1835,KUV 01024−138	21 969	66	7.642	0.011	2	
WD 0102−142	01:05:22.16	−13:59:12.8	15.93 B	MCT 0102−1414, PHL 980	19 945	29	7.858	0.005	2	
HE 0103−3253	01:05:30.77	−32:37:54.3	16.12 B		13 248	76	7.853	0.009	2	
WD 0103−278	01:05:53.52	−27:36:56.8	15.45	G 269−093, LTT 0615	14 410	2	7.789	0.005	2	
MCT 0105−1634	01:08:09.81	−16:18:44.5	16.44 B	PHL 997	28 212	130	7.835	0.021	2	
WD 0106−358	01:08:20.75	−35:34:43.0	14.74	MCT 0106−3550, GD 683	29 198	33	7.860	0.007	2	
HE 0106−3253	01:08:36.07	−32:37:43.5	15.34 B	(Ton S 193,SGPA 234)	17 234	25	7.999	0.005	2	
WD 0107−192	01:09:33.13	−19:01:19.2	16.18	GD 685, GR 563	14 304	78	7.788	0.013	2	
WD 0108+143	01:10:55.14	+14:39:21.3	16.40 B	G 033−045, LP 467−027	9217	20	8.530	0.026	2	
WD 0110−139	01:13:09.85	−13:39:35.8	15.68 B	MCT 0110−1355	24 692	55	7.990	0.007	2	

Table 1. continued.

Object	RA(2000)	Dec(2000)	mag(band)	Aliases	$T_{\rm eff}$ [K]	$\sigma(T_{\rm eff})$ [K]	$\log g$	$\sigma(\log g)$	Spectra	Remarks
MCT 0110−1617	01:13:14.12	−16:01:45.6	16.37 B		34 621	75	7.747	0.015	2	
MCT 0111−3806	01:14:03.23	−37:50:41.9	15.48 B		71 306	535	7.190	0.024	2	
WD 0112−195	01:15:05.62	−19:15:20.0	16.20 B	MCT 0112−1931	36 364	187	7.658	0.028	2	
WD 0114−605	01:16:19.55	−60:16:07.6	14.90 B	HK 22953−18	24 692	46	7.754	0.006	2	
WD 0114−034	01:16:58.80	−03:10:55.7	16.20 B	GD 821, GR 515	19 460	99	7.771	0.019	2	
WD 0124−257	01:26:55.90	−25:30:53.7	15.66 B	MCT 0124−2546, GD 1352	23 042	67	7.789	0.010	2	
WD 0126+101	01:29:24.38	+10:22:59.7	14.38	G 002−040, WOLF 72	8557	5	7.621	0.010	2	
WD 0127−050	01:30:23.06	−04:47:57.8	13.60	HE 0127−0503, G 271−081	16 718	23	7.784	0.005	2	
WD 0129−205	01:31:39.21	−20:19:59.1	14.64 B	MCT 0129−2035	19 950	46	7.885	0.008	2	
HS 0129+1041	01:31:45.54	+10:56:59.1	15.60 B	(NLTT 5061)	16 738	44	7.916	0.009	2	
HS 0130+0156	01:32:57.38	+02:11:32.6	16.00 B	(PHL 1026)	41 083	155	7.742	0.016	2	
HE 0130−2721	01:33:09.08	−27:05:45.0	16.08 B	(GD 1372, KUV 01308−2721)	21 880	45	7.902	0.007	2	
HE 0131+0149	01:34:28.46	+02:04:21.4	14.69 B	(PHL 1040)	15 228	34	7.745	0.007	2	DDs
WD 0133−116	01:36:13.39	−11:20:31.3	14.10	G 271−106, ZZ CETI	12 249	15	7.856	0.005	2	DAV
WD 0135−052	01:37:59.40	−04:59:44.9	12.84	G 271−115, LHS 1270	6942	10	7.081	0.010	2	DDd
MCT 0136−2010	01:38:31.67	−19:54:50.6	16.49 B	PHL 3537	8416	10	8.405	0.012	2	DDs
MCT 0138−4014	01:40:10.98	−39:59:24.6	16.37 B	HE 0138−4014	21 698	44	7.898	0.007	2	
WD 0137−291	01:40:16.79	−28:52:53.7	16.04 B	MCT 0137−2908, GD 1384	21 550	55	7.755	0.009	2	
WD 0138−236	01:40:28.15	−23:21:22.8	16.10 B	MCT 0138−2336, PHL 1100	36 897	297	7.627	0.039	2	
WD 0140−392	01:42:50.99	−38:59:06.9	14.37	MCT 0140−3914, SB 702	21 811	24	7.918	0.004	2	
WD 0143+216	01:46:41.34	+21:54:48.1	15.05	G 94−9, WOLF 82	9222	9	8.340	0.009	2	
WD 0145−221	01:47:21.76	−21:56:51.4	15.30	MCT 0145−2211, GD 1400	11 747	20	8.066	0.007	2	DAV
WD 0145−257	01:48:08.18	−25:32:44.1	14.51		25 915	37	7.858	0.005	2	
HS 0145+1737	01:48:21.51	+17:52:13.5	15.70 B		18 125	29	7.894	0.006	2	
HE 0145−0610	01:48:22.27	−05:55:36.5	16.45 B	(PHL 1166,BPSCS 22962−0027)	8613	10	8.017	0.013	3	
HE 0150+0045	01:52:59.22	+01:00:20.2	16.40 B	SDSS	12 625	95	7.705	0.026	1	NOV(3)
WD 0151+017	01:54:13.88	+02:01:23.5	15.00	G 073−004, G 159−012	12 440	25	7.836	0.008	2	NOV(2)
HE 0152−5009	01:54:35.98	−49:55:01.9	16.32 B	(CSI−50−01527,JL 265)	13 185	43	7.651	0.008	2	
WD 0155+069	01:57:41.33	+07:12:03.8	15.34	GD 20, FEIGE 17	22 007	56	7.668	0.008	2	
WD 0158−227	02:00:53.41	−22:27:35.7	16.00 B	HE 0158−224, PHL 1251	67 081	676	7.463	0.031	2	
HE 0201−0513	02:03:37.60	−04:59:12.8	15.94 B	(PB 9009,G 159−31)	24 626	102	7.638	0.013	1	
HS 0200+2449	02:03:45.80	+25:04:09.1	15.60 B		23 281	53	7.860	0.007	2	
WD 0203−138	02:05:49.05	−13:38:27.4	15.70 B		48 529	275	7.997	0.020	2	
WD 0204−233	02:06:45.10	−23:16:14.0	15.60	G 274−150, LP 829−017	13 095	78	7.775	0.010	2	
HE 0204−3821	02:06:47.55	−38:07:04.0	15.60 B		14 038	44	7.794	0.006	2	
HE 0204−4213	02:06:49.89	−41:59:25.8	16.43 B		22 575	58	7.902	0.009	2	
WD 0205−365	02:07:25.46	−36:20:49.4	16.10 B	MCT 0205−3635	61 240	448	7.742	0.024	2	
WD 0205−304	02:07:40.86	−30:10:59.6	15.67 B	GD 1442	17 209	31	7.761	0.006	2	
HE 0205−2945	02:08:08.00	−29:31:38.8	16.06 B		10 476	10	7.774	0.008	2	DDd
WD 0208−263	02:10:58.63	−26:07:01.3	15.80 B	HE 0208−2621	33 720	65	7.764	0.012	2	
HE 0210−2012	02:13:01.93	−19:58:35.2	16.29 B		17 612	27	7.800	0.006	2	
HE 0211−2824	02:13:56.66	−28:10:17.8	15.27 B		14 469	48	7.951	0.003	2	
WD 0212−231	02:14:21.26	−22:54:49.1	16.40 B	HE 0212−2308, GR 286	26 827	61	7.943	0.009	2	

Table 1. continued.

Object	RA(2000)	Dec(2000)	mag(band)	Aliases	$T_{\rm eff}$ [K]	$\sigma(T_{\rm eff})$ [K]	$\log g$	$\sigma(\log g)$	Spectra	Remarks
HS 0213+1145	02:16:07.61	+11:59:18.9	15.50 B		17 518	84	7.787	0.018	1	NOV
WD 0216+143	02:18:48.27	+14:36:03.2	14.58	PG 0216+144	26 637	29	7.791	0.005	2	DDs
HE 0219−4049	02:21:19.69	−40:35:29.7	16.20 B		15 373	36	7.893	0.005	2	
HE 0221−2642	02:23:29.40	−26:29:19.7	15.63 B		32 008	44	7.721	0.011	2	
WD 0220+222	02:23:36.07	+22:27:28.4	15.83	G 94−B5B, EG 18	15 630	65	7.890	0.010	1	
HE 0221−0535	02:23:59.88	−05:21:45.9	15.59 B	(PHL 1276)	24 747	49	7.954	0.007	2	
HE 0222−2336	02:24:19.89	−23:23:15.6	16.48 B		31 816	81	7.874	0.018	1	
HE 0222−2630	02:24:36.06	−26:16:52.2	15.59 B		23 198	38	7.911	0.005	2	
HS 0223+1211	02:26:29.98	+12:25:22.8	16.00 B		14 721	86	7.300	0.019	1	
HE 0225−1912	02:27:41.43	−18:59:24.5	16.14 B	(PHL 1295)	17 269	37	7.559	0.008	1	DDd
HS 0225+0010	02:27:55.50	+00:23:39.1	15.90 B		13 337	80	7.835	0.010	2	
WD 0226−329	02:28:27.70	−32:42:35.9	13.73 B	HE 0226−3255	22 294	22	7.875	0.003	3	
WD 0227+050	02:30:16.66	+05:15:50.7	12.65	Feige 22, EG 19	19 341	12	7.762	0.002	2	
WD 0229−481	02:30:53.31	−47:55:25.9	14.53	LB 1628, RE 0230−475	59 082	364	7.713	0.020	2	
WD 0231−054	02:34:07.73	−05:11:39.6	14.24	GD 31, PHL 1358	17 306	11	8.445	0.003	3	
HS 0237+1034	02:40:35.57	+10:47:01.5	16.00 B		17 259	70	7.857	0.015	1 DDs	
HS 0241+1411	02:44:00.75	+14:24:29.6	16.20 B		13 753	150	7.763	0.019	1	
WD 0242−174	02:45:02.35	−17:12:20.6	15.33	HK 22189−19	20 663	38	7.853	0.007	1	
WD 0243+155	02:46:24.06	+15:45:01.9	16.46 mc	PG 0243+155	17 611	61	7.958	0.013	1	
HE 0245−0008	02:47:46.45	+00:03:30.4	16.45 B	SDSS	18 813	115	7.977	0.022	1	
HE 0246−5449	02:48:07.16	−54:36:44.9	16.39 B		15 949	45	7.829	0.010	2	
WD 0250−026	02:52:51.05	−02:25:17.4	14.73	HE 0250−0237,KUV 02503−0238	15 315	23	7.797	0.005	2	
WD 0250−007	02:53:32.29	−00:33:45.3	16.40	KUV 02510-0046, SDSS	7948	13	7.793	0.019	2	
WD 0252−350	02:54:37.25	−34:49:56.6	15.89 B	HE 0252−3501	16 934	34	7.366	0.007	2	
WD 0255−705	02:56:16.90	−70:22:17.7	14.08	L 54−5, LFT 245	10 514	8	8.080	0.006	2	NOV(1)
HE 0255−1100	02:58:21.72	−10:48:25.7	15.99 B	(PB 9404)	20 827	132	7.836	0.020	1	
HE 0256−1802	02:58:59.54	−17:50:20.3	16.41 B		26 212	62	7.757	0.010	2	
HE 0257−2104	02:59:52.65	−20:52:49.6	16.30 B		17 362	42	7.692	0.008	2	
HE 0300−2313	03:02:36.69	−23:01:52.0	15.35 B		22 369	37	8.386	0.005	2	
WD 0302+027	03:04:37.40	+02:56:56.6	14.97	GD 41, FEIGE 31	35 270	61	7.772	0.009	2	
HE 0303−2041	03:06:04.96	−20:29:31.1	16.26 B	(PHL 1467)	10 006	10	8.131	0.010	2	
HE 0305−1145	03:08:10.25	−11:33:45.7	15.40 B	(PHL 8567)	26 822	68	7.812	0.010	2	
WD 0307+149	03:09:53.95	+15:05:22.1	15.10 B	HS 037+1454, PG 0307+149	21 413	27	7.909	0.004	2	
HS 0307+0746	03:10:09.13	+07:57:32.6	16.50 B		10 127	14	8.070	0.013	2	
WD 0310−688	03:10:30.99	−68:36:03.3	11.40	CPD−69°177, LB 3303	16 329	6	7.908	0.001	4	
HE 0308−2305	03:11:07.24	−22:54:05.6	15.16 B		23 565	41	8.538	0.006	2	
WD 0308+188	03:11:49.22	+19:00:55.5	13.86 B	PG 0308+188	18 450	21	7.725	0.004	2	
HS 0309+1001	03:12:34.96	+10:12:27.2	15.60 B		18 786	31	7.725	0.006	2	
WD 0315−332	03:17:26.05	−33:03:05.4	16.53 B	HE 0315−3314	49 926	350	7.472	0.025	3	
HS 0315+0858	03:17:43.18	+09:09:55.2	15.90 B		18 783	38	7.871	0.007	2	
HE 0315−0118	03:18:13.31	−01:07:13.1	14.71 B	SDSS	13 469	51	7.614	0.007	2	DDd
HE 0317−2120	03:19:27.22	−21:09:13.2	15.80 B		9688	13	8.093	0.014	2	
WD 0317+196	03:20:04.07	+19:47:35.4	15.58 B	PG 0317+196	17 735	50	7.776	0.011	1	

Table 1. continued.

Object	RA(2000)	Dec(2000)	mag(band)	Aliases	$T_{\rm eff}$ [K]	$\sigma(T_{\rm eff})$ [K]	$\log g$	$\sigma(\log g)$	Spectra	Remarks
WD 0318−021	03:20:58.77	−01:59:59.5	16.01	HE 0318−0210,KUV 03184−0211	15 125	45	7.702	0.008	2	
WD 0320−539	03:22:14.81	−53:45:16.3	14.99 B	LB 1663, RE J0322−534	32 588	28	7.769	0.006	3	
HE 0320−1917	03:22:31.91	−19:06:47.8	16.00 B	(PHL 4402)	13 248	88	7.168	0.016	2	DDs
HE 0324−2234	03:26:26.88	−22:24:15.0	16.39 B	(PHL 1537)	16 905	35	7.845	0.008	2	
HE 0324−0646	03:26:39.97	−06:36:05.2	15.95 B	BGK, SDSS	15 740	41	7.866	0.008	2	
HE 0324−1942	03:27:05.02	−19:32:23.8	16.25 B	(PHL 1541)	20 660	49	8.078	0.008	2	DDd
HE 0325−4033	03:27:43.92	−40:23:26.1	16.38 B		16 737	50	7.695	0.010	2	DDs
HS 0325+2142	03:28:25.24	+21:53:08.4	15.30 B		13 863	118	7.935	0.011	1	
WD 0326−273	03:28:48.81	−27:19:01.7	14.00	LP 888−064, L 0587−077A	9190	5	7.717	0.006	2	DDs
WD 0328+008	03:31:33.93	+01:03:26.5	16.80	HE 0328+0053, SDSS	34 476	113	7.920	0.022	2	
HE 0330−4736	03:32:03.98	−47:25:57.7	16.03 B		12 913	38	8.034	0.008	2	
HS 0329+1121	03:32:35.92	+11:31:31.9	15.80 B		17 376	85	7.855	0.018	1	
WD 0330−009	03:32:36.90	−00:49:36.6	15.74 B	HE 0330−0059,KUV 03301−0100	34 044	59	7.740	0.011	2	
HS 0331+2240	03:34:53.26	+22:50:07.8	15.00 B		21 452	54	7.783	0.009	1	
HE 0333−2201	03:36:02.77	−21:51:21.5	15.46 B	(PHL 4465)	16 046	47	8.192	0.005	1	
HE 0336−0741	03:38:26.79	−07:31:54.6	16.33 B		15 854	22	7.769	0.009	2	
WD 0336+040	03:38:56.21	+04:09:43.0	15.90	KUV 03363+0400	8703	12	7.828	0.018	3	
HS 0337+0939	03:39:58.55	+09:49:11.3	16.20 B		14 371	79	7.780	0.013	2	
					12 483	57	7.970	0.015	2	amb
HE 0338−3025	03:40:18.33	−30:15:36.0	16.25 B	(PHL 8735)	9959	9	8.131	0.010	2	
WD 0339−035	03:41:54.49	−03:22:40.9	15.20	GD 47, LP 653−026	14 759	27	7.780	0.004	2	NOV(1)
					12 415	20	7.940	0.005	2	amb
WD 0341+021	03:44:10.77	+02:15:29.9	15.30 B	HE 0341+0206, KUV 03416+0206	22 153	61	7.273	0.008	2	DDs
WD 0343−007	03:46:25.21	−00:38:39.4	14.91	KUV 0898−06, SDSS	62 994	563	7.677	0.028	2	
WD 0344+073	03:46:51.42	+07:28:01.9	16.10	KUV 03442+0719	10 474	14	7.748	0.012	3	DDs, NOV
HS 0344+0944	03:46:52.31	+09:53:56.1	16.50 B		15 321	205	8.227	0.028	1	
HE 0344−1207	03:47:06.71	−11:58:08.5	15.80 B		11 352	85	8.098	0.018	2	DAV
HS 0345+1324	03:48:39.58	+13:33:29.3	15.90 B		25 064	67	8.182	0.008	2	
HS 0346+0755	03:49:15.29	+08:04:53.6	16.30 B		16 796	70	7.720	0.014	2	
WD 0346−011	03:48:50.24	−00:58:33.2	13.99	GD 50, GR 288, SDSS	40 455	77	9.313	0.009	2	
HE 0348−4445	03:49:59.27	−44:36:27.4	16.22 B		19 951	39	8.069	0.007	2	
HE 0348−2404	03:50:38.82	−23:55:45.2	16.26 B		14 735	54	7.944	0.006	2	
HE 0349−2537	03:51:41.37	−25:28:16.6	15.74 B		20 974	44	7.906	0.008	2	
WD 0352+049	03:54:40.21	+05:08:45.5	16.20	KUV 03520+0500	37 253	124	8.611	0.020	1	
WD 0352+052	03:54:41.09	+05:23:19.4	15.90	KUV 03520+0515, GD54	10 136	14	7.967	0.014	2	
WD 0352+018	03:54:43.47	+01:58:41.4	15.63	HE 0352+0149, KUV 03521+0150	22 107	58	7.797	0.008	2	
WD 0352+096	03:55:22.02	+09:47:17.5	14.47	HS 0352+0938, HZ 4	14 440	47	8.178	0.005	2	
HE 0358−5127	03:59:38.30	−51:18:41.5	15.60 B		23 376	47	7.927	0.006	2	
HS 0400+1451	04:03:42.08	+14:59:28.9	15.10 B		14 623	61	8.250	0.005	2	
HS 0401+1454	04:04:35.02	+15:02:26.7	16.20 B		14 795	59	7.796	0.011	1	NOV
					12 527	49	7.965	0.013	1	amb
HE 0403−4129	04:05:30.11	−41:21:10.2	16.13 B		22 702	62	7.937	0.010	2	
HE 0404−1852	04:07:11.18	−18:44:33.5	16.00 B	(PPM 710547)	19 218	59	7.665	0.011	1	

Table 1. continued.

Object	RA(2000)	Dec(2000)	mag(band)	Aliases	$T_{\rm eff}$ [K]	$\sigma(T_{\rm eff})$ [K]	$\log g$	$\sigma(\log g)$	Spectra	Remarks
WD 0406+169	04:09:28.89	+17:07:54.0	15.35	GH 7−112, LP 414−101	16 049	48	8.236	0.008	1	
WD 0407+179	04:10:10.33	+18:02:24.0	14.14	HZ 10, HS 0407+1754	14 421	2	7.768	0.003	3	NOV(1)
WD 0408−041	04:11:02.17	−03:58:22.2	15.50	GD 56, GR 571	15 414	45	7.856	0.010	1	
HE 0409−5154	04:11:10.33	−51:46:50.8	15.48 B		26 315	67	7.830	0.009	2	
HE 0410−1137	04:12:28.99	−11:30:08.3	16.13 B	(GD 57)	17 406	34	7.601	0.007	2	DDd
WD 0410+117	04:12:43.60	+11:51:48.5	13.86	HS 0409+1144, HZ 2	21 074	22	7.843	0.004	2	
HS 0412+0632	04:14:58.36	+06:40:07.0	15.50 B	(GD 59)	13 290	52	7.812	0.006	2	
HE 0414−4039	04:16:02.87	−40:32:11.7	15.88 B		20 941	57	7.935	0.010	2	
WD 0416−550	04:17:11.51	−54:57:47.9	15.11 B	HE 0416−5505	30 547	51	7.118	0.011	2	
HE 0416−3852	04:18:04.14	−38:45:20.6	16.01 B		19 324	49	7.956	0.010	2	
HE 0416−1034	04:18:47.84	−10:27:09.6	15.83 B		24 845	35	7.917	0.005	2	
HE 0417−3033	04:19:22.07	−30:26:44.0	16.51 B		19 103	62	7.846	0.012	1	
HE 0418−5326	04:19:24.83	−53:19:17.4	16.38 B	(FAUST 545, FD 30)	27 090	66	7.872	0.011	2	
HE 0418−1021	04:21:12.03	−10:14:09.0	16.21 B		23 385	34	8.287	0.007	1	
WD 0421+162	04:23:55.81	+16:21:13.9	14.29	GH 7−191, VR 7	19 616	22	8.025	0.004	2	
HE 0423−2822	04:25:20.85	−28:15:19.9	16.54 B		10 907	21	8.066	0.012	3	NOV
HS 0424+0141	04:26:52.45	+01:47:47.7	15.60 B		44 174	212	7.679	0.019	2	
HE 0425−2015	04:27:39.77	−20:09:15.2	16.49 B		19 801	54	8.115	0.010	2	
WD 0425+168	04:28:39.48	+16:58:10.4	14.01	GH 7−233, VR 16	24 000	25	8.036	0.004	2	
HE 0426−1011	04:28:42.32	−10:04:48.9	16.07 B		18 386	21	7.854	0.004	2	
WD 0426+106	04:28:58.29	+10:44:48.7	16.30	KUV 04262+1038	10 058	26	8.407	0.020	2	
HE 0426−0455	04:29:26.32	−04:48:46.7	14.89 B		14 129	55	7.989	0.005	2	
WD 0431+126	04:33:45.08	+12:42:40.4	14.18	HS 0430+1236, HZ 7	21 374	28	7.968	0.005	2	
HE 0436−1633	04:38:47.33	−16:27:21.4	16.22 B		14 092	67	7.959	0.006	2	
WD 0437+152	04:39:52.97	+15:19:44.0	15.83	KUV 04370+1514	18 711	39	7.247	0.008	2	
WD 0440−038	04:43:07.07	−03:46:49.5	16.00		68 468	618	8.420	0.027	2	
WD 0446−789	04:43:46.67	−78:51:50.2	13.47	BPM 3523	23 627	22	7.687	0.003	2	
HE 0452−3429	04:54:05.85	−34:25:05.9	16.49 B		14 825	47	7.810	0.008	1	
HE 0452−3444	04:54:23.69	−34:39:48.7	15.86 B		21 206	40	7.839	0.007	2	
HE 0455−5315	04:56:58.35	−53:10:26.6	16.20 B		24 432	94	7.553	0.013	3	DDs
WD 0455−282	04:57:13.38	−28:07:53.6	13.95	RE 0457−280, EUVE J0457−281	54 386	155	7.682	0.010	2	
HE 0456−2347	04:58:51.47	−23:42:55.7	16.42 B		23 645	66	7.794	0.009	2	
HS 0503+0154	05:05:39.24	+01:58:28.2	15.20 B	(1RXS J050539.1+015825)	54 563	289	7.544	0.017	2	
HE 0507−1855	05:09:20.47	−18:51:17.3	16.38 B		20 421	48	8.271	0.008	2	
HS 0507+0434B	05:10:13.59	+04:38:54.0	15.36		11 488	18	8.057	0.008	2	DAV
HS 0507+0434A	05:10:14.01	+04:38:37.4	14.21		20 838	26	7.897	0.005	2	
HE 0508−2343	05:10:39.43	−23:40:10.1	16.24 B		16 811	64	7.738	0.014	2	
WD 0509−007	05:12:06.51	−00:42:07.2	13.90	RE 0512−004, EUVE J0512−007	31 910	29	7.294	0.007	2	
WD 0511+079	05:14:03.61	+08:00:14.5	15.89		6137	12	7.228	0.025	2	
WD 0510−418	05:12:23.03	−41:45:26.3	16.50		50 490	366	7.680	0.024	2	
HE 0516−1804	05:19:04.27	−18:01:29.1	16.14 B		12 976	103	7.765	0.017	1	
WD 0518−105	05:21:18.95	−10:29:17.4	15.89	RE 0521−102, EUVE J0521−104	32 008	44	8.818	0.010	2	
HE 0532−5605	05:33:06.70	−56:03:53.3	16.12 B	(EC 05321−5605)	11 285	21	8.454	0.007	2	DAV
WD 0548+000	05:50:37.62	+00:05:50.4	14.79	GD 257, GR 289	44 684	107	7.822	0.010	2	
WD 0549+158	05:52:27.63	+15:53:13.1	13.06	GD 71, LTT 11733	32 959	16	7.731	0.003	3	

Table 1. continued.

Object	RA(2000)	Dec(2000)	mag(band)	Aliases	$T_{\rm eff}$ [K]	$\sigma(T_{\rm eff})$ [K]	$\log g$	$\sigma(\log g)$	Spectra	Remarks
WD 0556+172	05:59:44.95	+17:12:03.9	15.79	KPD 0556+1712	18 825	31	8.094	0.006	2	
WD 0558+165	06:01:17.67	+16:31:37.2	15.69	KPD 0558+1631	16 807	27	8.183	0.005	2	
WD 0603−483	06:05:02.75	−48:19:59.8	16.00		34 731	61	7.842	0.012	2	
WD 0612+177	06:15:18.67	+17:43:40.1	13.39	G 104−27, LTT 11818	25 624	24	7.814	0.003	2	
WD 0621−376	06:23:12.71	−37:41:30.8	12.09	RE 0623−374, EUVE J0623−376	57 806	120	7.269	0.006	2	
WD 0628−020	06:30:38.59	−02:05:51.0	15.30 B	LP 600−42	6414	12	7.248	0.023	1	
WD 0630−050	06:32:57.79	−05:05:49.8	15.54	RE 0632−050, EUVE J0632−050	42 451	175	8.335	0.015	2	
WD 0642−285	06:44:28.77	−28:32:38.6	15.20 B	LP 895−041	9133	21	7.809	0.032	1	
WD 0646−253	06:48:56.20	−25:23:48.2	13.80		27 990	21	7.791	0.004	2	
WD 0659−063	07:01:55.00	−06:27:48.7	15.27	LHS 1892, LP 661−003	6046	7	7.019	0.016	2	
WD 0710+216	07:13:21.61	+21:34:06.8	15.29	GD 83, EG 214	10 206	9	7.990	0.008	2	NOV
WD 0715−704	07:15:17.00	−70:25:06.5	14.00		44 915	124	7.674	0.010	2	
WD 0721−276	07:23:20.06	−27:47:22.8	14.80		36 520	53	7.704	0.008	2	
WD 0732−427	07:33:37.84	−42:53:58.8	14.16	L 384−24, BPM 33039	14 995	28	8.000	0.005	2	
WD 0810−728	08:09:31.99	−72:59:17.2	15.15	RE 0809−725, EUVE J0809−729	30 598	32	7.845	0.007	3	
HS 0820+2503	08:23:46.21	+24:53:45.9	15.00 B	SDSS	33 367	80	7.660	0.014	2	
WD 0830−535	08:31:52.02	−53:40:33.7	14.46	RE 0831−534, EUVE 0831−536	30 050	20	7.763	0.004	3	
WD 0838+035	08:41:03.90	+03:21:16.1	15.20	SDSS	38 342	48	7.716	0.005	2	
WD 0839−327	08:41:32.62	−32:56:34.8	11.90	L 532−81, CD−32°5613	9174	3	7.828	0.004	2	
WD 0839+231	08:42:53.06	+23:00:25.8	14.42	PG 0839+232	25 852	39	7.636	0.005	2	
WD 0852+192	08:55:30.73	+19:04:37.8	15.70 B	LB 8888, HS 0852+1916	15 130	39	7.848	0.007	2	
WD 0858+160	09:01:33.46	+15:51:43.3	15.83	HS 0858+1603	16 064	34	7.774	0.008	2	
WD 0859−039	09:02:17.34	−04:06:56.3	12.40		23 731	14	7.792	0.002	3	
WD 0908+171	09:11:24.05	+16:54:11.5	16.06 mc	PG 0908+171, SDSS	17 640	33	7.830	0.007	2	
WD 0911−076	09:14:22.39	−07:51:25.6	16.16	EC 09119−0738	18 175	34	7.854	0.007	2	
WD 0916+064	09:18:41.87	+06:17:02.2	15.66 B	PG 0916+065, SDSS	43 048	232	7.368	0.021	1	
WD 0922+162B	09:25:13.22	+16:01:45.6	17.30		25 783	178	9.039	0.028	1	
WD 0922+162A	09:25:13.55	+16:01:44.7	16.26		23 537	48	8.226	0.008	3	
WD 0922+183	09:25:18.37	+18:05:34.3	16.46 mc	PG 0922+183	24 532	59	8.159	0.008	2	
WD 0928−713	09:29:08.65	−71:34:02.8	15.44	L 64−40, BPM05639	8389	6	8.057	0.009	3	
HS 0926+0828	09:29:36.53	+08:15:46.8	16.20 B	(SDSS)	14 939	65	7.700	0.013	2	NOV(3)
					12 027	51	7.911	0.015	2	amb
HS 0929+0839	09:32:29.85	+08:26:37.5	16.10 B	BGK	15 707	39	7.774	0.014	2	
HS 0931+0712	09:34:32.67	+06:58:48.2	16.50 B	SDSS	36 719	193	7.160	0.025	2	
HS 0933+0028	09:36:07.96	+00:14:35.9	16.00 B		32 219	69	8.100	0.016	2	
HS 0937+0130	09:39:58.67	+01:16:38.2	16.50 B	SDSS	19 717	47	8.314	0.008	2	
WD 0937−103	09:40:11.96	−10:34:25.1	15.97	EC 09377−1020	17 562	30	8.502	0.005	2	
WD 0939−153	09:41:56.22	−15:32:14.6	15.92	EC 09395−1518	13 500	58	7.787	0.007	2	
HS 0940+1129	09:43:14.38	+11:16:11.4	16.10 B		15 176	49	7.838	0.009	2	
					13 031	128	7.878	0.014	1	amb
HS 0943+1401	09:46:31.60	+13:47:35.8	16.40 B		16 863	25	8.275	0.010	2	
HS 0944+1913	09:47:31.67	+18:59:12.7	15.30 B		17 444	17	7.883	0.003	2	
HS 0949+0935	09:51:48.94	+09:21:12.6	16.30 B	(SDSS)	18 357	65	7.694	0.013	2	
HS 0949+0823	09:51:56.17	+08:09:33.7	16.10 B		14 755	66	7.808	0.012	2	NOV(3)
WD 0950+077	09:52:59.15	+07:31:08.3	16.12 B	PG 0950+078	15 623	37	7.891	0.006	2	

Table 1. continued.

Object	RA(2000)	Dec(2000)	mag(band)	Aliases	$T_{\rm eff}$ [K]	$\sigma(T_{\rm eff})$ [K]	$\log g$	$\sigma(\log g)$	Spectra	Remarks
WD 0951−155	09:53:40.36	−15:48:56.6	16.09	EC 09512−1534	17 973	33	7.827	0.007	2	
WD 0954+134	09:57:18.99	+13:12:57.0	16.41 B	PG 0954+135, SDSS	16 462	75	7.677	0.015	2	
WD 0955+247	09:57:48.37	+24:32:55.5	15.07	G49−33, LTT 12661	8446	6	7.985	0.009	2	
WD 0956+045	09:58:37.24	+04:21:31.0	15.80 mc	PG 0956+046	18 228	41	7.779	0.008	3	
WD 0956+020	09:58:50.49	+01:47:23.5	15.61 B	HE 0956+0201, PG 0956+021, SDSS	16 495	25	7.806	0.006	2	
WD 1000−001	10:03:16.34	−00:23:36.9	16.08 mc	PG 1000−002, LB 564	20 253	50	7.803	0.009	2	
WD 1003−023	10:05:51.54	−02:34:19.5	15.43	PG 1003−023	20 614	35	7.889	0.006	2	
HS 1003+0726	10:06:23.08	+07:12:12.6	15.30 B	SDSS	9486	16	8.020	0.018	1	
WD 1010+043	10:13:12.78	+04:05:12.8	16.34 B	PG 1010+043	28 617	56	7.903	0.010	2	
HE 1012−0049	10:15:11.75	−01:04:17.1	15.57 B	(2MASS)	23 204	47	8.074	0.007	2	
HS 1013+0321	10:15:48.15	+03:06:46.8	15.60 B	SDSS	11 600	24	7.983	0.010	2	DAV
WD 1013−010	10:16:07.01	−01:19:18.7	15.33	G 053−038, EG 253	8066	6	7.509	0.011	2	DDs
WD 1015−216	10:17:26.67	−21:53:43.4	15.66	EC 10150−2138	30 937	40	7.891	0.008	2	
WD 1015+076	10:18:01.69	+07:21:22.4	15.37	PG 1015+076	27 375	124	7.728	0.018	1	
WD 1015+161	10:18:03.84	+15:51:58.3	15.57 mc	PG 1015+161	19 948	33	7.925	0.006	2	
WD 1017−138	10:19:52.45	−14:07:35.5	14.56	EC 10174−1352, RE J1019−140	31 798	26	7.845	0.006	2	
WD 1017+125	10:19:56.02	+12:16:29.9	15.75 mc	PG 1017+125	21 386	43	7.875	0.007	2	
WD 1019+129	10:22:28.77	+12:41:59.4	15.60	PG 1019+129	18 412	29	7.885	0.006	2	
WD 1020−207	10:22:43.83	−21:00:02.1	15.09	EC 10203−2044	19 920	58	7.926	0.010	1	
WD 1022+050	10:24:59.90	+04:46:09.0	14.18	PG 1022+050, LP 550−52	14 693	55	7.364	0.012	1	DDs, NOV(2)
WD 1023+009	10:25:49.77	+00:39:04.4	16.40 mc	PG 1023+009	37 817	157	7.650	0.017	2	
WD 1026+023	10:29:09.87	+02:05:49.7	14.20 mc	PG 1026+024, LP 550−292	12 338	18	7.955	0.004	3	NOV(2)
WD 1031−114	10:33:42.79	−11:41:40.4	13.00	EC 10312−1126, L 0825−014	25 502	27	7.845	0.004	1	
WD 1031+063	10:34:05.43	+06:02:45.6	16.26 mc	PG 1031+063	21 317	67	7.759	0.010	2	
WD 1036+085	10:39:07.48	+08:18:39.1	16.07 B	PG 1036+086	22 924	93	7.324	0.012	2	
HS 1043+0258	10:46:23.34	+02:42:35.6	15.60 B	SDSS	13 739	74	7.756	0.010	2	
WD 1049−158	10:52:20.69	−16:08:05.9	14.36	EC 10498−1552	20 037	23	8.276	0.004	2	
WD 1053−550	10:55:13.77	−55:19:05.8	14.32	L 250−52, BPM 20383	14 621	20	7.857	0.004	2	NOV(1)
WD 1053−290	10:55:40.04	−29:19:53.4	15.38	EC 10532−2903	10 664	10	8.068	0.006	2	
WD 1053−092	10:55:45.41	−09:30:59.1	16.38 B	HE 1053−0914, PG 1053−092	22 620	61	7.694	0.009	2	
HS 1053+0844	10:55:51.54	+08:28:46.6	16.50 B		16 556	49	7.813	0.011	2	
WD 1056−384	10:58:20.19	−38:44:26.5	14.08	RE 1058−384, EUVE J1058−387	27 947	25	7.898	0.004	2	
WD 1058−129	11:01:12.28	−13:14:42.7	14.93	EC 10587−1258, PG 1058−129	23 892	32	8.651	0.005	4	
HS 1102+0934	11:04:36.76	+09:18:22.7	16.40 B	BGK, SDSS	16 961	55	7.367	0.012	3	DDs
WD 1102−183	11:04:47.08	−18:37:15.2	15.99	EC 11023−1821	8057	8	7.851	0.011	3	
HS 1102+0032	11:05:15.33	+00:16:26.3	14.80	(SDSS, GD 127)	12 610	49	8.242	0.011	2	NOV(3)
WD 1105−048	11:07:59.98	−05:09:27.3	12.92	LP 672−001, G 163−050	15 995	11	7.753	0.002	2	
HS 1115+0321	11:17:46.18	+03:04:51.3	15.40 B	BGK, SDSS, GD 131	14 267	39	7.709	0.007	2	
WD 1116+026	11:19:12.55	+02:20:30.9	14.57	GD 133, PG 1116+026	12 121	23	8.005	0.005	2	DAV
HE 1117−0222	11:19:34.66	−02:39:06.3	14.25 B	(GD 135)	14 709	36	7.978	0.005	2	
WD 1121+216	11:24:13.08	+21:21:34.8	14.23	G 120−45, LHS 304	6929	7	7.306	0.011	2	
WD 1122−324	11:24:35.62	−32:46:25.7	15.86	EC 11221−3229	21 671	38	7.855	0.006	2	
WD 1123+189	11:26:19.11	+18:39:17.2	14.01 mc	PG 1123+189, RE J1126+183	58 126	205	7.498	0.012	2	
HE 1124+0144	11:26:49.74	+01:27:56.4	16.30	BGK, SDSS	16 246	35	7.743	0.007	2	
WD 1124−293	11:27:09.32	−29:40:11.8	15.02	EC 11246−2923, ESO 0439−080	9397	6	8.099	0.007	2	
WD 1124−018	11:27:21.33	−02:08:37.7	16.47 mc	PG 1124−019, SDSS	23 942	45	7.628	0.009	2	DDs

Table 1. continued.

Object	RA(2000)	Dec(2000)	mag(band)	Aliases	$T_{\rm eff}$ [K]	$\sigma(T_{\rm eff})$ [K]	$\log g$	$\sigma(\log g)$	Spectra	Remarks
WD 1125−025	11:28:14.50	−02:50:27.3	15.32 B	PG 1125−026, RE J1128−025	31 755	36	8.159	0.008	2	
WD 1125+175	11:28:15.68	+17:14:06.9	15.95	PG 1125+175	61 213	484	7.490	0.027	2	
WD 1126−222	11:29:11.64	−22:33:44.4	16.17	EC 11266−2217	11 818	41	8.009	0.012	2	DAV
WD 1129+071	11:32:03.58	+06:55:07.9	14.90 mc	PG 1129+072	14 599	35	7.831	0.006	2	
WD 1129+155	11:32:27.46	+15:17:29.1	14.04 mc	PG 1129+156	17 739	16	8.029	0.003	2	
WD 1130−125	11:33:19.50	−12:49:01.2	15.50	EC 11307−1232	14 138	61	8.342	0.008	2	
HS 1136+1359	11:39:25.42	+13:43:11.0	16.00 B	(A1 117)	23 921	204	7.828	0.028	1	
HS 1136+0326	11:39:26.64	+03:10:19.7	16.20 B		13 530	126	7.926	0.017	2	
WD 1141+077	11:43:59.45	+07:29:04.7	14.11 B	PG 1141+078	62 493	345	7.554	0.018	1	
WD 1144−246	11:47:20.13	−24:54:56.7	15.71	EC 11448−2438	30 500	41	7.161	0.009	2	
HS 1144+1517	11:47:25.13	+15:00:38.7	16.30 B	BGK, SDSS	15 385	59	7.773	0.013	2	
WD 1145+187	11:48:03.18	+18:30:46.6	14.22	PG 1145+188, RE J1148+183	27 167	27	7.798	0.004	2	
WD 1147+255	11:50:20.18	+25:18:32.6	15.55	G 121−022, HS 1406+2229	9910	11	8.046	0.011	2	NOV(1)
WD 1149+057	11:51:54.29	+05:28:38.3	14.91 mc	PG 1149+058, SDSS	11 023	21	8.057	0.012	3	DAV
WD 1150−153	11:53:15.37	−15:36:36.8	16.00	EC 11507−1519	12 132	42	8.033	0.008	2	DAV
HE 1152−1244	11:54:34.91	−13:01:16.8	15.81 B		13 126	54	7.780	0.006	2	
WD 1152−287	11:54:45.82	−29:00:40.7	16.38	EC 11522−2843	20 620	79	7.628	0.013	1	
HS 1153+1416	11:55:59.76	+14:00:13.3	15.80	(PB 3724)	15 553	65	7.785	0.014	2	
WD 1155−243	11:57:33.65	−24:39:27.9	16.48	EC 11550−2422	13 831	96	7.888	0.011	2	
WD 1159−098	12:02:07.71	−10:04:40.8	15.97 mc	HE 1159−0947, LP734−006	9261	8	8.537	0.008	2	
WD 1201−001	12:03:47.53	−00:23:11.8	15.12 mc	HE 1201−006, SDSS	19 853	27	8.295	0.005	2	
WD 1202−232	12:05:26.80	−23:33:13.6	12.79	EC 12028−2316	8615	4	8.042	0.006	2	
WD 1204−322	12:06:47.63	−32:34:33.8	15.68	EC 12042−3217, HE 1204−3217	21 263	41	7.996	0.007	2	
WD 1204−136	12:06:56.43	−13:53:53.6	15.52	EC 12043−1337	10 939	16	8.190	0.008	2	NOV(4)
HS 1204+0159	12:07:29.51	+01:42:50.6	16.50 B		24 756	86	7.755	0.011	2	
WD 1207−157	12:10:09.34	−16:00:40.4	16.32	EC 12075−1543, HE 1207−1543	16 885	48	7.775	0.010	2	
WD 1210+140	12:12:33.89	+13:46:25.1	14.67		32 127	36	6.924	0.008	2	DDs
WD 1214+032	12:16:51.84	+02:58:04.3	15.32	LP 544−063, SDSS	6272	14	6.915	0.030	1	
HE 1215+0227	12:17:56.20	+02:10:45.8	16.35 B	(SDSS)	59 691	723	7.595	0.040	2	
WD 1216+036	12:18:41.15	+03:20:21.7	15.94 mc	PG 1216+036, SDSS	14 404	3	7.769	0.009	2	
WD 1218−198	12:21:07.35	−20:07:05.1	16.35	EC 12185−1950	35 013	81	7.912	0.015	2	
WD 1220−292	12:23:05.17	−29:32:28.9	15.79	EC 12204−2915	17 702	29	7.890	0.005	2	
HE 1225+0038	12:28:07.72	+00:22:19.6	15.09 B	(SDSS)	9383	5	8.094	0.005	3	
WD 1229−012	12:31:34.46	−01:32:08.5	14.24	HE 1229−0115, SDSS	19 540	21	7.500	0.004	2	
WD 1230−308	12:33:00.67	−31:08:36.4	15.81	EC 12303−3052	22 764	38	8.280	0.006	2	
WD 1231−141	12:33:36.89	−14:25:08.6	16.12	EC 12310−1408	17 217	35	7.923	0.007	2	
WD 1233−164	12:36:14.02	−16:41:53.5	15.10	EC 12336−1625	24 892	33	8.207	0.004	3	
WD 1236−495	12:38:50.02	−49:48:01.1	13.96	L 327−186, LTT 4816	11 372	12	8.743	0.004	2	DAV
WD 1237−028	12:40:09.66	−03:10:14.8	15.97 mc	PG 1237−029, SDSS	9936	13	8.421	0.012	2	
WD 1241+235	12:44:16.57	+23:14:10.8	15.18 mc	PG 1241+235, LB 16	26 982	50	7.772	0.008	2	
WD 1241−010	12:44:28.66	−01:18:59.6	14.00	PG 1241−010, SDSS	23 459	25	7.379	0.003	2	DDd
HS 1243+0132	12:45:38.74	+01:16:16.1	15.60 B	(UM 517,LEDA 43016)	21 644	65	7.817	0.010	2	
WD 1244−125	12:47:26.88	−12:48:42.0	14.70	EC 12448−1232	13 429	39	7.928	0.005	2	
HE 1247−1130	12:49:54.26	−11:47:00.2	14.74 B		28 110	62	7.840	0.011	2	
EC 12489−2750	12:51:41.08	−28:06:48.8	16.22		61 045	459	7.628	0.023	2	
HS 1249+0426	12:52:15.19	+04:10:43.0	15.80 B	(PB 4304)	11 382	19	8.029	0.009	2	DAV
WD 1249+160	12:52:17.15	+15:44:43.4	14.63	GD 150, SDSS	25 792	40	7.214	0.006	2	

Table 1. continued.

Object	RA(2000)	Dec(2000)	mag(band)	Aliases	$T_{\rm eff}$ [K]	$\sigma(T_{\rm eff})$ [K]	$\log g$	$\sigma(\log g)$	Spectra	Remarks
WD 1249+182	12:52:23.34	+17:56:53.9	15.48	GD 151	19 911	25	7.729	0.004	2	
HE 1252−0202	12:54:58.10	−02:18:36.7	16.50 B	(BGK, SDSS)	15 934	64	7.806	0.015	2	
WD 1254+223	12:57:02.33	+22:01:52.7	13.33	GD 153, BPM 88611, SDSS	39 537	42	7.587	0.005	2	
WD 1257+047	12:59:50.35	+04:31:26.6	14.99	GD 267, LP556−035, SDSS	21 759	32	7.949	0.005	2	
WD 1257+032	12:59:56.69	+02:55:56.2	15.60 B	PG 1257+032, PB 4421, SDSS	17 579	24	7.814	0.005	2	
HE 1258+0123	13:01:10.50	+01:07:39.9	16.42 B	(SDSS, 2MASS)	11 258	22	7.946	0.013	2	DAV
WD 1300−098	13:03:16.77	−10:09:12.5	16.25 B	PG 1300−099	15 327	63	8.143	0.008	2	NOV
HS 1305+0029	13:08:20.87	+00:13:30.5	16.20 B	BGK, SDSS	14 725	51	7.846	0.008	2	
HE 1307−0059	13:09:41.67	−01:15:05.9	15.72 B		18 191	45	7.907	0.009	2	
HS 1308+1646	13:11:06.06	+16:31:03.4	15.50 B		10 727	15	8.242	0.011	2	NOV
WD 1308−301	13:11:17.52	−30:25:57.6	15.11	EC 13085−3010	14 422	33	7.899	0.004	2	
HE 1310−0337	13:13:28.35	−03:53:19.7	16.31 B		18 943	73	7.825	0.013	1	
WD 1310−305	13:13:41.59	−30:51:33.7	14.48	EC 13109−3035	20 353	22	7.819	0.004	3	
EC 13123−2523	13:15:03.94	−25:39:01.0	15.69		75 463	825	7.682	0.027	1	
WD 1314−153	13:16:43.59	−15:35:58.7	14.86	EC 13140−1520, LHS 2712	16 152	25	7.720	0.005	3	
WD 1314−067	13:17:18.46	−06:59:28.1	15.87 B	PG 1314−067	16 832	52	7.847	0.011	2	
HE 1315−1105	13:17:47.29	−11:21:06.2	15.76 B		9067	7	8.103	0.009	2	
WD 1323−514	13:26:09.62	−51:41:37.9	14.60	L 258−46, L 257−47	19 357	22	7.765	0.004	2	
HE 1325−0854	13:28:23.90	−09:09:53.0	15.14 B		17 021	16	7.810	0.004	2	
HE 1326−0041	13:29:24.69	−00:56:43.9	16.27 B		18 671	55	7.841	0.011	2	
WD 1326−236	13:29:24.92	−23:52:18.1	15.97	EC 13266−2336	13 808	85	7.919	0.010	2	
WD 1327−083	13:30:13.58	−08:34:30.2	12.31	G 014−058, BD−07D3632	14 699	8	7.791	0.001	3	
HE 1328−0535	13:31:20.03	−05:50:52.4	16.34 B		36 420	137	7.872	0.020	2	
WD 1328−152	13:31:34.82	−15:30:48.0	15.49	EC 13288−1515,HE 1328−1515	61 253	285	7.719	0.015	2	
WD 1330+036	13:33:17.80	+03:21:00.2	15.86	GD 269, BPM 89123, SDSS	17 408	26	7.831	0.005	2	
WD 1332−229	13:35:10.47	−23:10:38.3	16.30	EC 13324−2255	20 264	49	7.859	0.008	2	
HS 1334+0701	13:36:33.67	+06:46:26.8	15.00 B		16 891	43	7.270	0.009	2	DDs
WD 1334−160	13:36:59.29	−16:19:44.1	15.32	EC 13342−1604, L 0762−021	18 653	21	8.316	0.004	2	
WD 1334−678	13:38:08.11	−68:04:37.4	15.57	L 106−73, LHS 2769	8769	8	7.929	0.012	2	
HE 1335−0332	13:38:22.72	−03:47:19.5	16.47 B		20 188	75	8.470	0.013	2	
HS 1338+0807	13:41:27.63	+07:52:29.5	16.00 B		24 440	188	7.649	0.024	1	
HE 1340−0530	13:43:17.88	−05:45:35.8	16.40 B		32 936	141	7.911	0.024	2	
WD 1342−237	13:45:46.58	−23:57:11.0	16.06	EC 13429−2342	10 988	19	8.092	0.011	2	DAV
WD 1344+106	13:47:24.45	+10:21:36.6	15.08	G 063−054, LHS 2800	6480	7	7.079	0.015	2	
WD 1348−273	13:51:22.84	−27:33:59.1	15.00	LP 846−53, LTT 5382	9835	9	8.039	0.008	3	
WD 1349+144	13:51:54.06	+14:09:44.2	15.34	PG 1349+114, PB 4117	16 925	28	7.642	0.006	2	DDd
WD 1356−233	13:59:07.97	−23:33:28.7	14.96	EC 13563−2318	9498	6	8.100	0.007	2	
WD 1401−147	14:03:57.16	−15:01:10.4	15.67	EC 14012−1446	11 768	23	8.080	0.008	2	DAV
WD 1403−077	14:06:04.86	−07:58:31.0	15.82	PG 1403−077,EUVE J1406−07.9	49 033	253	7.810	0.017	2	
WD 1410+168	14:12:27.89	+16:35:40.5	15.70 B	LP 439−387	21 323	40	7.756	0.007	2	
HS 1410+0809	14:13:06.56	+07:55:23.5	15.50 B		16 217	142	8.370	0.020	2	
WD 1411+135	14:13:58.22	+13:19:19.3	16.20	US 3969	18 562	55	8.108	0.011	2	
WD 1412−109	14:15:07.75	−11:09:24.2	15.86 mc		26 226	52	7.814	0.007	2	
HE 1413+0021	14:16:00.21	+00:07:59.3	16.03		14 544	81	8.114	0.011	2	
HE 1414−0848	14:16:52.07	−09:02:03.8	16.15 B		9823	7	7.867	0.010	2	DDd

Table 1. continued.

Object	RA(2000)	Dec(2000)	mag(band)	Aliases	$T_{\rm eff}$ [K]	$\sigma(T_{\rm eff})$ [K]	$\log g$	$\sigma(\log g)$	Spectra	Remarks
WD 1418−088	14:20:54.82	−09:05:08.7	15.36	G 124−026	8003	10	7.911	0.013	2	
WD 1420−244	14:23:26.25	−24:43:29.4	16.24	EC 14205−2429	20 917	40	8.159	0.007	2	
WD 1422+095	14:24:39.24	+09:17:12.7	14.32	GD 165, L 1124−010	12 525	21	7.917	0.007	2	DAV
WD 1426−276	14:29:27.38	−27:51:01.3	15.92	EC 14265−2737	18 087	28	7.661	0.006	2	
HE 1429−0343	14:32:03.15	−03:56:37.8	15.84 B		11 199	27	8.041	0.015	2	DAV
HS 1430+1339	14:33:05.47	+13:26:32.4	16.10 B		10 012	12	8.321	0.014	2	
WD 1425−811	14:33:08.92	−81:20:12.6	13.75	L 19−2, BPM 00784	12 069	17	7.916	0.003	2	DAV
WD 1431+153	14:34:06.80	+15:08:17.9	15.80 B	HS 1431+1521, PG 1431+153	13 941	72	7.883	0.008	2	NOV(1)
HS 1432+1441	14:35:20.85	+14:28:41.3	16.00 B	BGK, SDSS, GD 167	16 204	42	7.748	0.009	2	
WD 1434−223	14:37:14.74	−22:31:16.0	16.37	EC 14343−2218	27 690	138	7.374	0.021	1	
HE 1441−0047	14:44:33.85	−00:59:59.5	16.40 B	(SDSS)	15 775	72	8.025	0.014	2	NOV(3)
HS 1447+0454	14:50:09.91	+04:41:45.7	15.60 B		13 926	38	7.820	0.005	2	
WD 1448+077	14:50:49.46	+07:33:32.9	15.46	G 136−022, LP 561−013	14 921	30	7.686	0.006	2	
WD 1449+168	14:52:11.37	+16:38:03.5	15.44	PG 1449+168	22 346	46	7.785	0.007	2	
WD 1451+006	14:53:50.48	+00:25:29.3	15.19	GD 173, GR 297, SDSS	25483	31	7.891	0.004	2	
WD 1457−086	14:59:52.99	−08:49:29.5	15.77	EC 14572−0837, PG 1457−086	21448	54	7.917	0.009	2	
WD 1500−170	15:03:14.45	−17:11:56.7	15.27	EC 15004−1700	31 757	23	7.926	0.005	2	
WD 1501+032	15:04:23.92	+03:02:30.5	15.43 mc	PG 1501+032	14 741	50	7.932	0.007	2	
WD 1503−093	15:06:19.44	−09:30:20.9	15.15	EC 15036−0918	12 681	20	8.032	0.005	2	
WD 1507+220	15:09:39.99	+21:50:15.5	15.00 B	PG 1507+220	19 872	27	7.745	0.005	3	
WD 1507+021	15:09:56.98	+01:56:07.5	16.49	PG 1507+021, SDSS	20 222	67	7.796	0.012	1	
WD 1507−105	15:10:29.08	−10:45:19.8	15.42	GD 176	10 063	8	7.663	0.008	2	NOV(1)
HE 1511−0448	15:14:12.97	−04:59:33.9	15.41 B	(PG 1511−048)	50 899	126	7.447	0.009	4	DDs
WD 1511+009	15:14:21.31	+00:47:52.3	15.87	PG 1511+009, LB 769	28 041	48	7.822	0.009	2	
WD 1515−164	15:18:35.07	−16:37:29.2	16.03	EC 15157−1626	14 248	62	7.969	0.003	2	
HS 1517+0814	15:20:06.00	+08:03:27.4	15.90 B	BGK, SDSS	14 494	44	7.761	0.008	2	
HE 1518−0344	15:20:46.03	−03:54:52.2	16.03 B		28 493	50	7.808	0.009	2	
HE 1518−0020	15:21:30.87	−00:30:54.7	15.25 B		15 392	29	7.820	0.006	2	
HE 1522−0410	15:25:12.26	−04:21:29.3	16.36 B		10 357	12	8.130	0.012	2	
HS 1527+0614	15:29:41.47	+06:04:01.9	15.90 B		14 925	39	7.769	0.007	2	
WD 1527+090	15:29:50.41	+08:55:46.6	14.29	PG 1527+091	21 197	27	7.846	0.005	2	
WD 1524−749	15:30:36.64	−75:05:24.2	15.93	L 72−91, BPM 9518	23 091	40	7.743	0.006	3	
WD 1531+184	15:33:49.31	+18:18:55.4	16.20	GD 186	13 625	104	7.774	0.013	1	NOV(1)
WD 1531−022	15:34:06.08	−02:27:07.3	14.03	GD 185, BPM 77964	19 234	18	8.354	0.004	2	
WD 1532+033	15:35:09.96	+03:11:13.9	16.02	PG 1532+034	61 907	327	7.761	0.018	2	
WD 1537−152	15:40:23.77	−15:23:43.2	15.90	EC 15375−1514	16 954	29	7.942	0.006	2	
WD 1539−035	15:42:14.15	−03:41:31.4	15.20	GD 189, PG1539−035	9875	6	8.246	0.006	2	
WD 1543−366	15:46:58.23	−36:46:44.1	15.81	RE 1546−364, EUVE J1546−367	42 701	119	8.974	0.012	2	
WD 1544−377	15:47:30.00	−37:55:08.8	12.72	CD−37°6571B,L 481−060	10 547	5	8.089	0.003	2	NOV(1)
WD 1547+057	15:49:34.93	+05:35:15.9	15.92	PG 1547+057	24 355	58	8.355	0.007	2	
WD 1547+015	15:49:44.93	+01:25:55.1	15.90 mc	PG 1547+016	76 588	591	7.497	0.022	2	
WD 1548+149	15:51:15.52	+14:46:58.3	15.06 mc	PG 1548+149	21 452	46	7.857	0.007	2	
WD 1550+183	15:52:26.38	+18:10:18.8	14.83	GD 194, LTT 14705	14 860	72	8.248	0.007	2	NOV(1)
WD 1555−089	15:58:04.83	−09:08:06.9	14.80	G 152−B4B, EG 174	14 531	62	7.944	0.004	2	NOV(1)

Table 1. continued.

Object	RA(2000)	Dec(2000)	mag(band)	Aliases	$T_{\rm eff}$ [K]	$\sigma(T_{\rm eff})$ [K]	$\log g$	$\sigma(\log g)$	Spectra	Remarks
WD 1609+135	16:11:25.67	+13:22:17.1	15.10	G 138−008, LHS 3163	9256	6	8.560	0.007	2	
WD 1609+044	16:11:49.11	+04:19:38.0	15.22	PG 1609+045	29 593	22	7.791	0.005	2	
HS 1609+1426	16:12:06.51	+14:19:05.8	16.10 B		14 387	45	7.821	0.008	3	
WD 1614+136	16:16:52.31	+13:34:21.5	15.24	PG 1614+137	22 015	30	7.211	0.005	2	
WD 1614+160	16:17:08.79	+15:54:37.8	16.08 B	PG 1614+160	17 961	25	7.815	0.005	2	
HS 1614+1136	16:17:09.44	+11:29:01.8	16.40 B		13 644	174	8.000	0.019	1	
WD 1614−128	16:17:28.02	−12:57:45.6	15.00	G 153−040, LTT 6494	16 293	25	7.750	0.005	2	
WD 1615−154	16:17:55.24	−15:35:52.7	13.40	G 153−041, LP 744−040	29 465	14	8.031	0.003	2	
HS 1616+0247	16:19:18.91	+02:40:14.1	16.00 B		18 468	35	7.957	0.007	2	
WD 1619+123	16:22:03.92	+12:13:32.0	14.57 mc	PG 1619+123	16 853	29	7.685	0.006	2	
WD 1620−391	16:23:33.87	−39:13:47.9	10.97 mc	CD−38°10980	24 677	10	7.927	0.001	2	
WD 1625+093	16:27:53.57	+09:12:14.8	16.14	G 138−031,GR 327	6380	8	7.425	0.016	2	
WD 1636+057	16:38:54.53	+05:40:40.1	15.76	G 138−049, LHS 3230	8428	11	8.392	0.014	2	
WD 1640+113	16:42:54.87	+11:16:40.6	16.03	PG 1640+114	19 718	40	7.854	0.008	2	
HS 1641+1124	16:43:54.12	+11:18:50.2	16.10 B		12 323	40	7.951	0.011	2	
HS 1646+1059	16:48:40.74	+10:53:52.8	16.10 B		19 890	50	7.782	0.008	2	
HS 1648+1300	16:51:02.78	+12:55:12.7	15.60 B		18 693	28	7.785	0.006	2	
WD 1655+215	16:57:09.84	+21:26:48.4	14.04	G 169−34, LHS 3524	9204	6	8.034	0.007	2	
HS 1705+2228	17:07:08.03	+22:24:30.0	14.40 B		15 702	31	7.749	0.006	2	
WD 1716+020	17:18:35.27	+01:56:51.4	14.26	WOLF 672A, G 019−020	13 644	39	7.645	0.004	2	NOV(2)
WD 1733−544	17:37:00.76	−54:25:56.9	15.80	L 270-37, LTT 6999	6165	7	7.233	0.015	2	
WD 1736+052	17:38:41.72	+05:16:06.3	15.89	GR 140−002, GR 371	8838	7	8.063	0.010	3	
WD 1755+194	17:57:38.92	+19:24:18.5	15.91 mc	GD 370, GR 548	24 439	41	7.804	0.006	3	
WD 1802+213	18:04:23.53	+21:21:02.5	15.77 mc	GD 372, GR 496	16 787	46	7.645	0.010	2	
WD 1824+040	18:27:13.13	+04:03:45.9	13.90	G 021−015, ROSS 137	14 787	15	7.460	0.003	4	DDs
WD 1826−045	18:29:09.87	−04:29:36.5	14.57	G 021−016, L 0993−018	9057	8	7.993	0.010	1	
WD 1827−106	18:30:39.60	−10:37:00.9	14.25	G 155−019, EG 177	13 670	39	7.561	0.007	2	NOV(1)
					12 697	13	7.683	0.006	2	amb
WD 1834−781	18:42:25.50	−78:05:06.4	15.45	L 44−95, BPM 11593	17 723	22	7.772	0.005	2	
WD 1840+042	18:43:25.83	+04:20:20.6	14.92	GD 215, EG 225	8769	6	8.114	0.008	2	
WD 1845+019	18:47:37.00	+01:57:30.0	12.96	KPD 1845+0154	29 754	16	7.817	0.003	2	DDs
WD 18444-223	18:47:56.57	−22:19:37.9	13.90		32 443	27	7.985	0.005	2	
WD 1857+119	18:59:49.27	+11:58:39.8	15.52	G 141−054, EG 128	9868	11	8.006	0.011	3	
WD 1911+135	19:13:38.77	+13:36:26.3	14.00	G 142−B2A, EG 130	13 783	75	7.870	0.008	2	NOV(1)
WD 1914+094	19:16:50.53	+09:34:46.5	15.43	KPD 1914+0929	32 525	33	7.850	0.007	4	
WD 1914−598	19:18:44.85	−59:46:33.5	14.39	HK 22891−122	19 756	29	7.837	0.005	2	
WD 1918+110	19:20:35.29	+11:10:43.3	16.23	GD 218	19 268	43	7.809	0.008	2	
WD 1919+145	19:21:40.51	+14:40:40.5	12.94	GD 219, BPM 94172	15 252	13	8.007	0.002	2	
WD 1932−136	19:35:42.05	−13:30:07.8	15.95	L 852−037, LP 753−005	16 931	36	7.730	0.008	2	
WD 1943+163	19:45:31.73	+16:27:38.8	13.99	G 142−50, LTT 15765	19 763	23	7.791	0.004	2	
WD 1948−389	19:52:19.69	−38:46:13.6	14.63	HK 22964−60	37 199	64	7.751	0.010	2	
WD 1950−432	19:53:47.72	−43:07:13.6	14.86	MCT 1950-4314	40 835	135	7.602	0.013	2	
WD 1952−206	19:55:46.99	−20:31:02.9	15.00	L 709−20, LTT 7873	13 814	40	7.818	0.005	2	NOV(1)

Table 1. continued.

Object	RA(2000)	Dec(2000)	mag(band)	Aliases	$T_{\rm eff}$ [K]	$\sigma(T_{\rm eff})$ [K]	$\log g$	$\sigma(\log g)$	Spectra	Remarks
WD 1952−584	19:56:12.99	−58:20:49.0	16.06	HK 22873−42	33 509	61	7.752	0.011	2	
WD 1953−715	19:58:38.64	−71:23:43.6	15.15	L 80−56, LTT 7875	19 267	25	7.873	0.005	2	
WD 1959+059	20:02:12.92	+06:07:35.4	16.41	GD 226	10 846	15	8.070	0.010	2	DAV
WD 2004−605	20:09:05.83	−60:25:43.9	13.33	RE 2009−602, EUVE J2009−604	40 994	60	8.393	0.006	2	
WD 2007−219	20:10:17.48	−21:46:46.0	14.40	L 710−30, LTT 7983	9788	6	8.073	0.006	2	
WD 2007−303	20:10:56.82	−30:13:06.7	12.18	LTT 7987	15 436	9	7.803	0.002	2	
WD 2014−575	20:18:54.88	−57:21:33.8	13.00	RE 2018−572, EUVE J2018−573	26 804	27	7.929	0.003	2	
WD 2018−233	20:21:28.71	−23:08:30.4	14.40 B	HK 22955−37	15 585	29	7.808	0.006	2	
WD 2020−425	20:23:59.57	−42:24:26.7	14.87	RE 2023−422, EUVE J2024−424	28 412	26	8.145	0.005	2	DDd
WD 2021−128	20:24:42.94	−12:41:48.4	14.20 B	HK 22950−122	20 753	61	7.820	0.011	1	
WD 2029+183	20:32:02.91	+18:31:15.1	16.31	GD 230	13 525	77	7.647	0.008	2	NOV(1)
WD 2032+188	20:35:13.84	+18:59:21.8	15.34	GD 231, BPM 95701	18 199	28	7.355	0.005	2	DDs
WD 2039−202	20:42:34.64	−20:04:35.6	12.33	LTT 8189, L 711−010	19 738	10	7.786	0.002	2	
WD 2039−682	20:44:21.35	−68:05:21.4	13.25	L 116−79, LTT 8190	16 943	12	8.336	0.002	2	
HS 2046+0044	20:48:38.26	+00:56:00.8	15.90 B		27 096	32	8.153	0.005	3	
WD 2046−220	20:49:46.18	−21:54:43.1	15.48	HK 22880−124	23 413	37	7.828	0.005	2	
WD 2051+095	20:53:43.18	+09:41:14.5	16.20 B	LP 516−013, HS 2051+0929	15 274	30	7.790	0.007	2	
HS 2056+0721	20:58:45.03	+07:33:37.5	15.30 B		27 289	42	8.321	0.007	1	
WD 2056+033	20:58:46.84	+03:31:49.4	16.26	PG 2056+033	51 835	252	7.696	0.016	2	
HS 2058+0823	21:01:13.36	+08:35:09.1	14.70 B	(1RXS J210113.4+083517)	36 844	57	7.780	0.009	2	
WD 2058+181	21:01:16.50	+18:20:55.4	15.00	GD 232, GR 279	17 349	23	7.754	0.005	3	
HS 2059+0208	21:01:47.77	+02:20:27.6	16.50 B		18 641	54	7.840	0.011	2	
WD 2059+190	21:02:02.68	+19:12:57.5	16.36	G 144−51, GR 377	6215	12	6.969	0.030	2	
HS 2108+1734	21:10:59.52	+17:46:32.8	15.20 B	(1RXS J211057.6+174712)	28 812	37	8.309	0.008	2	
WD 2115+010	21:17:33.58	+01:15:47.1	15.60	PG 2115+011	25 815	39	7.755	0.005	2	
WD 2115−560	21:19:36.60	−55:50:15.6	14.28	L 212−19, BPM 27273	9625	7	8.011	0.007	2	
WD 2120+054	21:22:34.98	+05:42:38.8	16.38	PG 2120+055	35 559	79	7.681	0.011	2	
WD 2122−467	21:25:30.19	−46:30:36.8	16.13 B	HE 2122−4643	16 334	37	8.054	0.008	3	
WD 2124−224	21:27:43.21	−22:11:48.9	14.70		47 780	149	7.707	0.010	2	
HS 2130+1215	21:33:01.47	+12:28:30.4	16.30 B	SDSS	32 995	89	7.738	0.016	2	
HS 2132+0941	21:34:50.91	+09:55:19.0	15.80 B		13 204	71	7.720	0.008	2	
HE 2133−1332	21:36:16.18	−13:18:33.0	13.94 B		9851	5	7.796	0.005	2	
WD 2134+218	21:36:36.15	+22:04:32.8	14.45	GD 234, EG 227	18 001	19	7.864	0.004	2	
WD 2136+229	21:38:46.21	+23:09:20.9	15.25	G 126−18, GR 582	10 084	11	8.060	0.009	1	NOV(1)
HE 2135−4055	21:38:49.70	−40:41:28.9	13.43 B	(NLTT 51713)	19 211	17	7.959	0.003	2	
WD 2137−379	21:40:18.48	−37:42:46.7	16.03 B	HE 2137−3756	21 013	46	7.855	0.008	2	
HS 2138+0910	21:41:03.02	+09:23:45.4	15.90 B		9263	7	7.883	0.010	2	
WD 2139+115	21:41:28.37	+11:46:22.1	15.80	GD 235, GR 280	15 551	28	7.794	0.007	2	
HE 2140−1825	21:43:42.73	−18:11:32.6	16.04 B		13 950	39	7.751	0.006	2	
WD 2146−433	21:49:38.96	−43:06:14.4	15.81	HK 22951−67	62 792	388	7.230	0.020	2	
HS 2148+1631	21:51:14.54	+16:45:23.1	15.90 B		16 776	34	7.793	0.007	2	
HE 2148−3857	21:51:19.23	−38:43:04.5	16.27 B		26 758	96	8.015	0.014	1	
WD 2149+021	21:52:25.43	+02:23:17.8	12.72	G 093−048, EG 150	17 926	9	7.862	0.002	2	
WD 2150+021	21:53:30.29	+02:23:11.6	16.40	PG 2150+021	40 874	158	7.659	0.016	2	
WD 2152−045	21:54:41.18	−04:18:18.0	15.00 B	HK 22965−20	19 837	36	7.380	0.006	3	
WD 2151−307	21:54:53.38	−30:29:19.6	14.82 B	RE 2154−302, EUVE J2154−304	28 580	26	8.273	0.005	2	

Table 1. continued.

Object	RA(2000)	Dec(2000)	mag(band)	Aliases	$T_{\rm eff}$ [K]	$\sigma(T_{\rm eff})$ [K]	$\log g$	$\sigma(\log g)$	Spectra	Remarks
WD 2152−548	21:56:21.32	−54:38:24.1	14.50		45 171	121	7.878	0.009	2	
WD 2153−419	21:56:35.32	−41:42:17.0	15.89	HE 2153−4156, RE J2156−414	46 503	177	7.939	0.015	2	
WD 2154−061	21:57:29.92	−05:51:54.8	15.10 B	HK 22965−8, PB 7026	36 259	85	7.744	0.012	2	
HE 2155−3150	21:58:46.08	−31:36:06.5	16.06 B		16 302	40	7.833	0.009	2	
WD 2157+161	21:59:34.35	+16:25:39.0	16.20	GD 272, GR 282	19 188	31	7.889	0.006	3	
HE 2159−1649	22:02:20.82	−16:34:38.3	15.90 B		19 486	34	7.841	0.006	2	
WD 2159−414	22:02:28.57	−41:14:30.6	15.88	HE 2159−4129,EUVE J2202−41.2	54 343	219	7.707	0.015	2	
WD 2200−136	22:03:35.63	−13:26:49.9	15.36	HE 2200−1341	24 734	47	7.611	0.006	2	DDd
WD 2159−754	22:04:21.27	−75:13:25.9	15.06	LHS 3572, BPM 14525	8911	6	8.622	0.008	2	
HE 2203−0101	22:06:02.44	−00:46:33.5	15.82 B	(PB 5070)	18 047	33	7.871	0.007	2	
WD 2204+071	22:07:16.20	+07:18:36.0	15.86	PG 2204+071	24 454	39	7.950	0.005	3	
WD 2205−139	22:08:29.60	−13:41:13.2	15.08	HE 2205−1355	25 231	32	8.246	0.004	3	
WD 2207+142	22:09:47.19	+14:29:46.6	15.61	G 018−034, LTT 16482	7229	20	7.603	0.032	2	
HE 2209−1444	22:12:18.05	−14:29:48.0	15.32 B	Kawka06, NLTT 53177	8290	0	8.191	0.030	1	DDd
HS 2210+2323	22:12:53.48	+23:38:00.4	15.70 B		23 233	47	8.238	0.006	2	
WD 2211−495	22:14:11.93	−49:19:27.1	11.70	RE 2214−491, EUVE J2214−493	62 336	181	7.544	0.007	2	
HS 2216+1551	22:18:57.15	+16:06:56.9	15.70 B		17 112	29	7.872	0.006	2	DDd
HE 2218−2706	22:21:23.91	−26:50:55.2	14.89 B		15 039	30	7.795	0.005	2	
HE 2220−0633	22:22:44.44	−06:17:54.9	15.97 B	(PHL 243)	15 523	38	7.885	0.007	2	
HS 2220+2146B	22:23:01.64	+22:01:31.0	15.00 B		18 743	44	8.241	0.008	2	
HS 2220+2146A	22:23:01.74	+22:01:25.0	15.00 B		14 601	32	8.080	0.012	1	
WD 2220+133	22:23:13.95	+13:38:55.5	15.60	PG 2220+134, SDSS	22 583	29	8.299	0.005	3	
HE 2221−1630	22:24:17.51	−16:15:47.0	16.18 B	(PHL 5103)	9937	9	8.161	0.008	2	
HS 2225+2158	22:28:11.47	+22:14:15.1	15.30 B		25 989	43	7.856	0.006	2	
WD 2226+061	22:29:08.66	+06:22:46.3	14.70	GD 236, LP 580−021	16 429	29	7.655	0.006	2	
WD 2226−449	22:29:19.47	−44:41:39.4	15.50	HK 22960−99	13 923	21	7.743	0.003	3	
HS 2229+2335	22:31:45.45	+23:51:23.9	15.60 B		19 300	38	7.900	0.007	2	
HE 2230−1230	22:33:38.69	−12:15:30.4	16.08 B	(PHL 315, GD 237)	20 949	41	7.807	0.007	2	
HE 2231−2647	22:34:02.59	−26:32:21.1	14.96 B		21 592	41	7.700	0.006	2	
HS 2233+0008	22:36:03.20	+00:07:23.9	13.90 B	(PHL 329)	24 529	22	7.989	0.003	2	
WD 2235+082	22:37:35.56	+08:28:48.5	15.42	PG 2235+082	36 519	49	7.734	0.007	4	
HE 2238−0433	22:41:04.90	−04:18:09.1	14.30 B	(PHL 372)	17 542	116	8.178	0.023	2	
HS 2240+125B	22:42:30.33	+12:50:02.2	16.50 B		13 935	112	7.989	0.012	2	
HS 2240+125A	22:42:31.14	+12:50:04.7	16.20 B		15 636	9	7.857	0.008	2	
WD 2240−045	22:42:44.62	−04:14:15.1	15.21	GD 240, FEIGE 106	44 102	107	7.721	0.010	2	
WD 2240−017	22:43:04.76	−01:27:53.6	16.17	G 028−013, PHL 386	9114	10	8.050	0.013	2	
WD 2241−325	22:44:43.23	−32:19:43.7	15.97 B	HE 2241−3235, PHL 396	32 316	32	7.945	0.007	2	
HS 2244+2103	22:46:45.28	+21:19:47.7	15.70 B		24 113	60	7.889	0.008	2	
HS 2244+0305	22:47:22.35	+03:21:45.8	16.20 B	(PB 5160)	60 460	413	7.540	0.023	2	
HE 2246−0658	22:48:40.05	−06:42:44.2	14.14 B	(PB 7225)	11 371	50	8.186	0.02	1	
WD 2248−504	22:51:02.02	−50:11:31.8	14.96	L 285−14, BPM 28016	16 336	37	7.737	0.007	2	
HE 2251−6218	22:54:59.62	−62:02:10.2	15.89 B		18 033	44	7.827	0.009	2	
WD 2253−081	22:55:49.49	−07:50:03.3	16.50	G 156−064,BD−08° 5980B	6211	13	6.926	0.026	3	
WD 2254+126	22:56:46.26	+12:52:49.9	16.00 B	GD 244, LP 521−049	11 707	23	7.989	0.009	3	DAV

Table 1. continued.

Object	RA(2000)	Dec(2000)	mag(band)	Aliases	$T_{\rm eff}$ [K]	$\sigma(T_{\rm eff})$ [K]	$\log g$	$\sigma(\log g)$	Spectra	Remarks
HS 2259+1419	23:01:55.18	+14:36:00.5	15.80 B	BGK, SDSS	13 816	57	7.743	0.007	2	
					12 672	30	7.821	0.009	2	amb
WD 2303+017	23:06:13.09	+01:58:51.6	15.76 B	PG 2303+017, PHL 400	40 977	112	7.667	0.011	3	
WD 2303+242	23:06:17.70	+24:32:07.5	15.29	PG 2303+243, KR Peg	11 147	11	8.018	0.006	2	DAV
WD 2306+130	23:08:30.58	+13:19:22.7	15.10	PG 2306+131, KUV 23060+1303	13 513	51	7.826	0.006	2	NOV(1)
WD 2306+124	23:08:35.07	+12:45:39.0	15.23	PG 2306+125, KUV 23061+1229	20 360	38	7.993	0.006	2	
WD 2308+050	23:11:18.05	+05:19:27.9	16.02	PG 2308+050, PB 5280	36 062	68	7.606	0.010	2	
WD 2309+105	23:12:21.71	+10:47:02.8	13.00	GD 246, BPM 97895	57 007	136	7.816	0.007	2	
WD 2311−260	23:13:53.20	−25:48:49.0	16.05 B	GD 1636, TON S094	51 160	332	7.772	0.021	2	
WD 2312−356	23:15:34.95	−35:24:51.8	15.20 B	HK 22888−32	15 122	21	7.818	0.004	3	
WD 2314+064	23:16:50.36	+06:41:27.6	15.93 mc	PG 2314+064, PB 5312	17 981	30	7.875	0.006	2	
HE 2315−0511	23:18:04.31	−04:54:45.7	15.37 B	(PHL 444)	33 451	82	7.721	0.014	3	
WD 2318+126	23:20:31.30	+12:58:14.5	16.10 B	HS 2318+1241, LP 582−41	13 788	59	7.803	0.008	2	
WD 2318−226	23:21:26.43	−22:20:22.5	16.05	GD 1648, PHL 475	29 851	50	7.890	0.011	2	
WD 2321−549	23:24:30.85	−54:41:35.5	15.20	HE 2321−5458, RE J2324−544	43 583	94	7.783	0.008	2	
WD 2322+206	23:24:35.22	+20:56:33.9	15.59	PG 2322+207, HS 2322+2040	12 636	28	7.842	0.006	2	NOV(1)
WD 2322−181	23:25:18.40	−17:51:57.8	15.38 B	G 273−040, LP 822−081	21 683	35	7.900	0.006	2	
WD 2324+060	23:26:44.55	+06:17:41.4	15.33 mc	PG 2324+060, PB 5379	16 261	20	7.827	0.005	2	
WD 2326+049	23:28:47.74	+05:14:53.5	13.10	G 029−038, LTT 16907	11 485	8	8.071	0.002	2	DAV
WD 2328+107	23:30:41.79	+11:02:05.0	15.53	PG 2328+108, KUV 23282+1046	22 390	30	7.778	0.004	2	
WD 2329−332	23:32:10.90	−33:01:08.1	16.26 B	HE 2329−3317, GD 1670	20 457	70	7.914	0.012	2	
WD 2330−212	23:32:59.48	−20:57:12.1	16.25 B	HE 2330−2113, PHL 559	26 442	69	7.443	0.010	2	DDs
WD 2331−475	23:34:02.32	−47:14:27.6	13.42	RE 2334−471, EUVE J2334−472	51 573	94	7.875	0.006	2	
WD 2333−165	23:35:36.59	−16:17:42.5	13.80 B	GD 1192, BPM 82758	13 303	19	7.875	0.003	2	
WD 2333−049	23:35:53.96	−04:42:14.8	15.65	G 157−082	10 608	12	8.040	0.009	2	NOV
HE 2334−1355	23:37:30.38	−13:38:33.4	15.64 B	(GD 1207, PB 7713)	30498	27	7.288	0.006	2	
WD 2336−187	23:38:52.78	−18:26:11.9	15.60 P	G 273−097, GR 557	7774	9	7.492	0.014	2	DDd
WD 2336+063	23:38:58.25	+06:35:28.6	15.60 mc	PG 2336+063, PB 5486	17 012	20	8.025	0.004	2	
MCT 2343−1740	23:46:25.63	−17:24:10.2	16.12 B	GD 1324	21 827	104	7.883	0.015	2	
HE 2345−4810	23:47:46.16	−47:53:42.8	15.99 B		29 352	35	7.324	0.007	2	DDs
MCT 2345−3940	23:48:26.42	−39:23:47.4	16.06 B		19 197	46	7.866	0.008	2	
WD 2347+128	23:49:53.51	+13:06:12.5	16.05	G 030−020, GR 405	10 874	19	7.999	0.011	2	DAV
WD 2347−192	23:50:02.96	−18:59:21.9	16.03	MCT 2347−1916, GD 1248	26 272	49	7.941	0.007	2	
HE 2347−4608	23:50:32.90	−45:51:34.8	16.20 B		17 738	33	7.304	0.007	2	
WD 2348−244	23:51:22.10	−24:08:17.0	15.33	EC 23487−2424	11 406	14	8.040	0.006	2	DAV
MCT 2349−3627	23:52:08.16	−36:10:40.1	16.41 B		44 455	265	7.877	0.022	2	
WD 2349−283	23:52:23.18	−28:03:15.9	15.54 B	MCT 2349−2819, PHL 578	17 427	24	7.730	0.005	2	
WD 2350−248	23:53:03.79	−24:32:03.1	15.21 B	MCT 2350−2448, PHL 580	28 867	26	8.375	0.005	2	
WD 2350−083	23:53:27.63	−08:04:39.5	16.18 mc	G 273−B1B, GR 558	18 529	37	7.790	0.007	2	
WD 2351−368	23:54:18.82	−36:33:55.1	15.10 B	L 505−42, LP 936−025	14 438	28	7.869	0.005	2	
MCT 2352−1249	23:55:13.68	−12:32:55.1	16.49	PHL 584, PB 8098	40 294	351	7.952	0.040	2	
WD 2353+026	23:56:27.70	+02:57:06.0	15.83	PG 2353+027, PB 5617	61 740	286	7.590	0.016	2	
WD 2354−151	23:57:33.44	−14:54:09.1	15.02 B	MCT 2354−1510, PHL 599	34 984	40	7.195	0.007	2	
HE 2356−4513	23:58:57.83	−44:57:13.5	15.38 B		17 418	17	7.861	0.004	3	

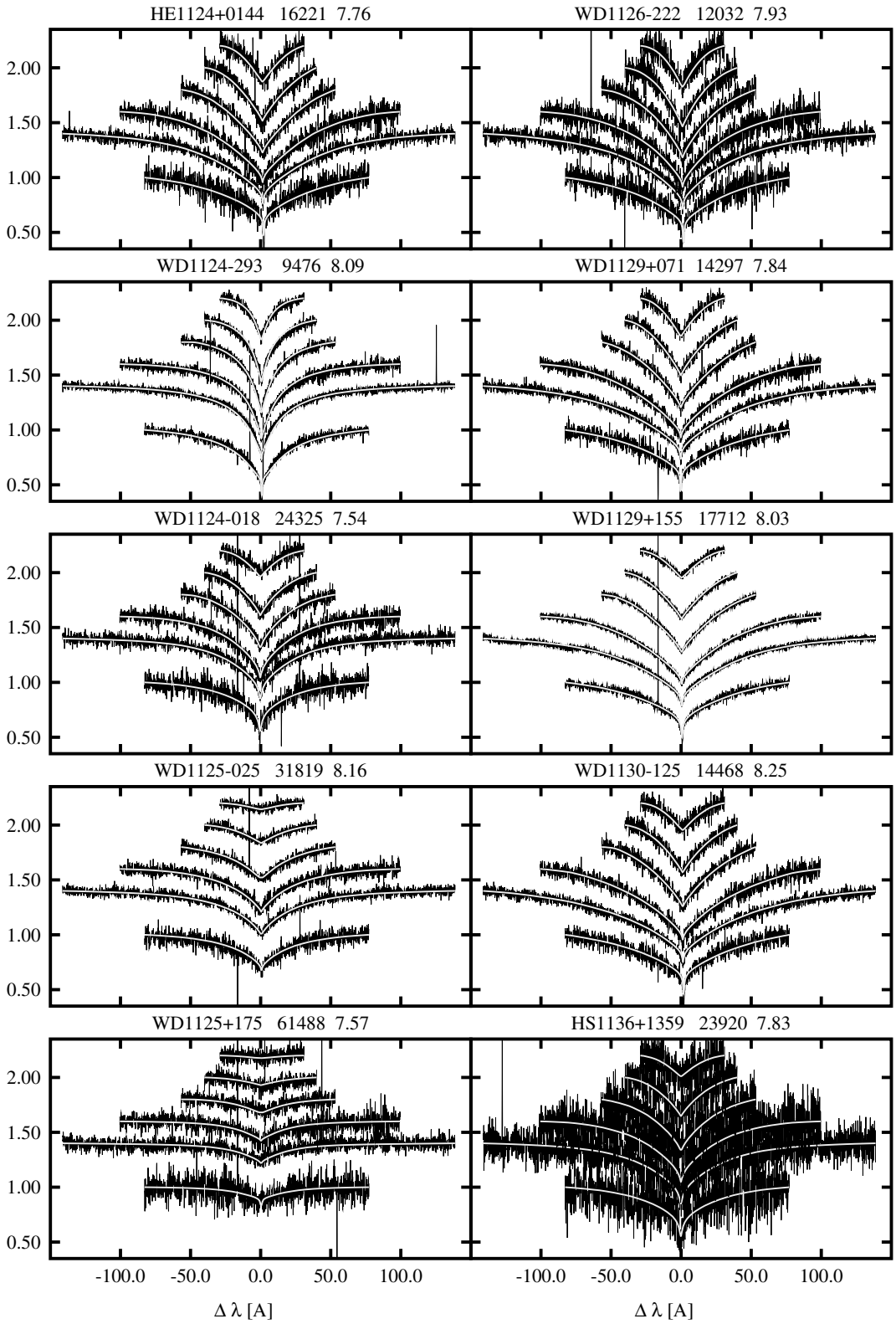

Fig. 1. Typical example for observations and fit, taking arbitrarily the entries 301 to 310 from Table 1. The header of each panel gives the name, effective temperature, and surface gravity of the fit. Shown are the six lowest Balmer lines. Vertical axis is relative intensity in arbitrary units, higher lines are offset for clarity. The light grey lines are the models.

of Liebert et al. (2005), the remaining standard deviations are $\sigma(T_{\rm eff}) = 2.3\%$, and $\sigma(\log g) = 0.08$. These values should be taken as indicative of the *statistical* errors of our results, and are compatible with the estimates derived above for the internal uncertainties from multiple spectra within our sample.

The surprisingly large systematic shift in surface gravity is unsatisfactory. A similar trend was also noted by Liebert et al. (2005) in their comparison with studies by other authors. In four out of five cases their $\log g$ was higher by 0.06−0.10 dex. Three of these used similar models to those used

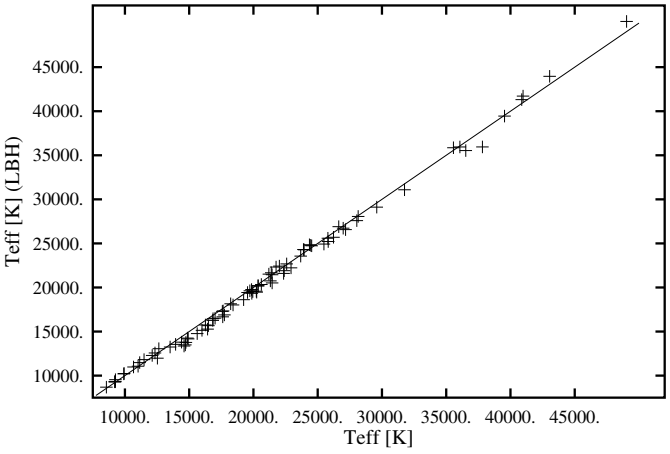

Fig. 2. Comparison of effective temperatures from this work with the results of Liebert et al. (2005), (=LBH) for 85 objects in common.

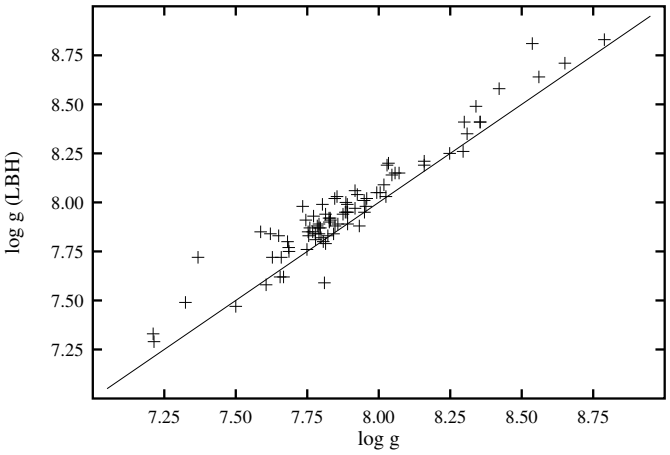

Fig. 3. Comparison of surface gravities from this work with the results of Liebert et al. (2005), (=LBH) for 85 objects in common.

here, and the differences could arise from differences between the "Bergeron" and the "Koester" models, or from the fitting procedures used. We are, however, not aware of any obvious explanations for such differences. Systematic differences of this magnitude were also found by Napiwotzki et al. (1999) in a comparison of different studies using low-resolution spectra.

A possible reason for systematic differences may also come from the nature of our observational data. The main purpose of the SPY was the determination of radial velocities, which needed high resolution; therefore the echelle spectrograph UVES was used. The wavelength interval per order ranges from ≈30 Å in the blue to ≈50 Å in the red region. Thus, e.g. Hα at maximum strength will extend over six or more orders, which have to be flatfielded and merged, removing the strong sensitivity change within orders. A real flux calibration was not possible, but the quality of the spectra obtained after some reprocessing of the ESO pipeline results was still very impressive. Before the start of this project, we were not certain that the spectra would be useful for anything else except radial velocity determinations.

Nevertheless, the merging of the orders and the approximate flux calibration attempted may have left very subtle artifacts influencing the far wings of the strong lines, thus influencing in particular the surface gravity results. An indication for this is visible in Table 1 in Koester et al. (2001), which compares the results of fits to echelle vs. single-order low-resolution spectra for the same seven DAs. The average surface gravity is lower by 0.07 in the results from the echelle spectra. Another hint towards this effect can be found in the study of low-resolution SDSS spectra of brighter DA white dwarfs by Koester et al. (2009), which used the same models and fitting routines as this work. The average surface gravity for 578 DAs with magnitude $g < 19$, $S/N > 10$, and 8000 K $\leq T_{\rm eff} \leq$ 16 000 K is 8.014, while the value from our current sample for the same temperature range is 7.947 from 211 objects. These are not the same objects of course, but the samples are so large, that the difference is significant.

Also marked in Table 1 are known ZZ Ceti variables (DAV), as well as objects, which have been observed photometrically, but were not found to vary (NOV). The references for the NOV designations are: (1) Gianninas et al. (2005); (2) Kepler et al. (1995); (3) Mukadam et al. (2004); and (4) Bergeron et al. (2004). If no reference is given the classification is a result of the SPY and/or follow-up observations (Voss 2006; Voss et al. 2006; Castanheira et al. 2006; Silvotti et al. 2005). We have not marked candidates for variability studies, but obviously all objects in the range of $T_{\rm eff}$ 10 000−13 000 K are interesting in this respect.

The Balmer lines reach their maximum strength near $T_{\rm eff}$ = 13 000, the exact value depending on the surface gravity. Therefore quite often two different fitting solutions exist, which produce the same overall strength (i.e. equivalent width) of the lines. The χ^2 values of the two minima are often similar, since model and observation are fitted in the far line wings and differences show up only in the inner core of the line. Visual inspection is usually sufficient to determine the correct solution. In a few cases, however, the difference was so small that we preferred to give both solutions in Table 1.

Because of the selection of the targets – as mentioned in the introduction – our sample is not well suited for a study of white dwarf population characteristics such as the mass distribution. However, it can be used to demonstrate an effect well known for many years (Bergeron et al. 1990a; Bergeron 1992; Kleinman et al. 2004; Eisenstein et al. 2006; Kepler et al. 2007; DeGennaro et al. 2008; Koester et al. 2009). This is the fact that the surface gravity seems to increase around $T_{\rm eff} \approx$ 12 000 K towards lower temperatures. Figure 4 clearly shows this for 465 objects between 7500 and 25 000 K. Taking the direct averages without any weighting we find $\langle \log g \rangle = 7.86$ for effective temperatures above 12 500 K and $\langle \log g \rangle = 8.06$ below. This is very similar to the results in the SDSS (Data Release 4) as studied by Koester et al. (2009). A number of possible explanations is discussed in that study, and the most likely is found to be an inadequate description of convection with the mixing-length approximation. However, this problem is certainly not yet solved.

4. Double-degenerate white dwarfs

Two or more spectra were taken for the vast majority of the SPY targets. Close binaries among them could be detected with a high level of confidence by checking for radial velocity variations indicating orbital motion. A total of 36 close binaries were detected among DA sample presented here from the spectra taken for the SPY. This count includes only the double degenerates, i.e. systems consisting of two white dwarfs. The DA+dM systems listed in Table 3 are not included in this count. Seventeen of the double-degenerates are double-lined, i.e. spectral lines of both white dwarfs are present in the spectra. The white dwarf companion in the single-lined systems is already so cool and faint that it does not produce a significant contribution to the combined spectrum.

Table 2. Magnetic or helium-contaminated hydrogen-rich stars.

Object	RA(2000)	Dec(2000)	mag(band)	Aliases	Remarks
WD 2359−434	00:02:10.73	−43:09:55.3	13.05	L362 −81, LHS 1005	DAP
HS 0051+1145	00:54:18.25	+12:01:59.9	15.60	(PHL 886)	DAH
WD 0058−044	01:01:02.25	−04:11:11.2	15.38	GD 9, GR 407	DAH
HS 0209+0832	02:12:04.90	+08:46:50.1	13.90		DAB
WD 0239+109	02:42:08.54	+11:12:31.8	16.18	G 004−034, LTT 10886	DAH
WD 0257+080	02:59:59.24	+08:11:55.3	15.90	LHS 5064, G 76−48	DAH
HS 1031+0343	10:34:30.14	+03:27:36.0	16.50 B		DAH
HE 1233−0519	12:35:37.58	−05:35:36.7	16.48		DAH
WD 1953−011	19:56:29.21	−01:02:32.2	13.69	G 092−040, L 0997−021	DAH
WD 2051−208	20:54:42.76	−20:39:25.9	15.06	HK 22880−134	DAH
WD 2105−820	21:13:16.52	−81:49:14.3	13.50	L 24−52, LTT8381	DAH

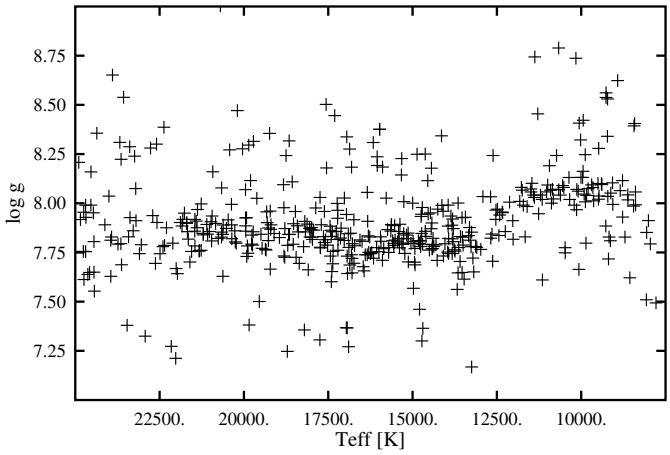

Fig. 4. Distribution of surface gravities for all objects between $T_{\rm eff}$ 7500−25 000 K.

Four more double-degenerates are marked in Table 1 as DD, but were found by independently obtained observations: HE 1511-0448 (Nelemans et al. 2005), WD 1241-010 (Marsh et al. 1995), WD 1022+050 and WD 2032+188 (Morales-Rueda et al. 2005).

The fitting procedure for the model atmosphere analysis is not affected by the binary nature of the single-lined binaries. The resulting fit parameters are those of the visible bright component. The situation is different for the double-lined systems. In these cases a deconvolution of simultaneous fit of both components would be necessary for accurate parameters. We have tools for this kind of analysis available (Napiwotzki et al. 2004), but in most cases more than the two spectra taken during the survey are needed to derive reliable parameters of both components. Here we present the results of a fit assuming a single star. Although these have to be taken with a pinch of salt, they are still a useful indication of the nature of properties of the binary. Double-lined systems are indicated in Table 1.

5. Objects with magnetic fields or helium contamination

Table 2 summarizes the data for some objects, which appear hydrogen-rich with some peculiarities, either Zeeman splitting of the Balmer lines due to a magnetic field or helium lines in addition to the stronger Balmer lines. For most of the stars we obtained fits with pure hydrogen model atmospheres. Since these are obviously not very reliable, we do not publish the parameters here, but discuss these stars individually.

Four magnetic DA stars in the SPY sample have not been published before, HS 0051+1145, HE 1233−0519, HS 1031+0343, and WD 2051−208. Two more objects were published first as DAH stars in Koester et al. (2001), WD 0058−044 and WD 0239+109. Four more magnetic DA, already described in the literature, are in the sample. Below, these ten objects and some additional white dwarfs of special interest are discussed.

HS 1031+0343. This object is a new magnetic DA star. The only Zeeman triplet that is completely present, and for which the three components are well discernible, is that of Hβ. The σ^-, π, σ^+ components are found at 4771 Å, 4851 Å, and 4905 Å. The components of the higher lines are blended together, and the σ^+ component of Hα is shifted by an amount that places it outside of the observed spectral range; thus only the σ^- and π components of Hα are available in the SPY data, at 6560 Å and 6420 Å. The magnetic field is estimated as $B = 6.1 \pm 0.3$ MG.

WD 0058−044. This star has been published as a magnetic DA by Koester et al. (2001). The shifts of the σ components with respect to the π components are 6.2 ± 0.3 Å and 3.6 ± 0.3 Å, for Hα and Hβ, respectively. The components of the higher Balmer lines are blended. The quadratic splitting of the lines is negligible here since the split is small and thus the field strength has to be low. The field is $B = 330 \pm 30$ kG, from Hα, and $B = 310 \pm 20$ kG, from Hβ.

WD 0239+109. Greenstein & Liebert (1990) recognized an unusual line shape for this object, and suggested a magnetic field as one of the possible reasons. Bergeron et al. (1990b) interpreted the spectrum as that of an unresolved DA+DC binary. The SPY spectra in Koester et al. (2001) revealed the presence of Zeeman splitting of Hα and thus proved the magnetic nature of the object. In the first SPY spectrum, the Hα components are placed at 6576.6 Å, 6562.3 Å, and 6548.4 Å, and those of Hβ at 4868.9 Å, 4861.0 Å, 4853.0 Å, and from that field strengths of 700 ± 20 kG, from Hα, and 720 ± 30 kG, from Hβ, can be derived.

WD 0257+080. Bergeron et al. (1997) found a flat-bottom Hα core for this object which is typical for white dwarfs with a low-strength magnetic field, but they were not able to identify a Zeeman triplet and estimated the field strength to be ∼100 kG. One of the two SPY spectra of WD 0257+080 clearly shows an Hα triplet. In the other spectrum, which has a slightly lower S/N,

Table 3. Data for DA+dM binaries. In boldface are the new SPY detections. For explanations of the magnitude column see text.

Object	RA(2000)	Dec(2000)	mag(band)	Aliases	Type
HE 0016−4340	00:19:06.10	−43:24:18.5	15.62 B		DA2
WD 0034−211	00:37:24.99	−20:53:43.6	14.53	MCT 0034−2110, LP 852−559	DA3
HE 0105−0232	01:08:06.33	−02:16:53.1	15.77 B	(PB6272)	DA2
WD 0131−163	01:34:24.08	−16:07:08.2	13.98	MCT 0131−1622, PHL 1043	DA1
WD 0137−349	01:39:42.88	−34:42:39.1	15.33	HK 29504−36	DA3
WD 0205+133	02:08:03.59	+13:36:23.9	13.78 B	PG 0205+134	DA1
WD 0232+035	02:35:07.67	+03:43:55.6	12.25	Feige 24	DA1
WD 0303−007	03:06:07.21	−00:31:14.3	16.21	HE 0303−0042, KUV 03036−0043	DA2
WD 0308+096	03:10:54.90	+09:49:31.6	15.23	PG 0308+096	DA2
HE 0331−3541	03:33:52.53	−35:31:18.9	14.79 B		DA2
WD 0347−137	03:50:14.55	−13:35:13.5	14.00	GD 51, LP 713−034	DA3
HE 0409−3233	04:11:21.14	−32:26:14.9	16.03 B		DA3
WD 0429+176	04:32:23.76	+17:45:02.4	13.93	GH 7−255, HZ9B	DA3
WD 0430+136	04:33:10.59	+13:45:12.4	16.50	KUV 04304+1339	DA1
HE 0523−3856	05:25:28.11	−38:54:12.5	16.07 B		DA3
WD 0718−316	07:20:47.92	−31:47:04.6	15.10	RE 0720−314, EUVE J 0720−317	DAO
WD 0933+025	09:35:40.69	+02:21:59.6	16.01 B	PG 0933+026	DA2
WD 0950+185	09:52:45.80	+18:21:02.9	15.30	PG 0950+186	DA2
WD 1001+203	10:04:04.30	+20:09:22.5	15.35	TON 1150, HS1001+2023	DA2
WD 1026+002	10:28:34.88	−00:00:29.6	13.89 B	PG 1026+002, HE 1026+014	DA3
WD 1042−690	10:44:10.63	−69:18:22.9	13.09	BPM 06502, L 101−080	DA2
WD 1049+103	10:52:27.82	+10:03:36.5	15.83 B	PG 1049+103	DA3
HE 1103−0049	11:06:27.66	−01:05:14.9	16.30 B		DA3
HE 1208−0736	12:11:01.08	−07:52:42.9	15.67 B		DA2
WD 1247−176	12:50:22.13	−17:54:48.2	16.19	EC 12477−1738, HE 1247−1738	DA3
WD 1319−288	13:22:40.46	−29:05:35.0	15.99	EC 13198−2849	DA5
HE 1333−0622	13:36:19.64	−06:37:58.9	16.05	WD 1333−063	DA2
WD 1334−326	13:37:50.77	−32:52:22.5	16.34	EC 13349−323	DA1
HE 1346−0632	13:48:48.34	−06:47:21.0	16.27 B		DA2
EC 13471−125	13:49:51.95	−13:13:37.5	14.80	WD 1347−129, RXS	DA3
WD 1415+132	14:17:40.22	+13:01:48.6	15.29	US 3974, Feige 93	DA1
EC 14329−162	14:35:45.70	−16:38:17.0	14.89	WD 1432−164, HE 1432−1625	DA3
WD 1436−216	14:39:12.70	−21:50:14.6	15.94	EC 14363−2137, HE 1436−2137	DA2
WD 1458+171	15:00:19.36	+16:59:14.7	16.12 B	PG 1458+172	DA5
WD 1541−381	15:45:10.97	−38:18:51.3	14.90	LDS 539B, L 480−085	DA4
HS 1606+0153	16:08:55.22	+01:45:48.6	15.00 B		DA3
WD 1643+143	16:45:39.05	+14:17:42.0	15.38	PG 1643+144	DA2
WD 1646+062	16:49:07.83	+06:08:43.6	15.84 B	PG 1646+062	DA2
WD 1845+019	18:47:39.09	+01:57:33.5	12.95	LAN 18, KPD 1845+0154	DA2
WD 1844−654	18:49:02.00	−65:25:14.2	15.80 B	HK 22959−81	DA1
HS 2120+0356	21:23:09.53	+04:09:28.3	16.20 B		DA3
HE 2123−4446	21:26:41.88	−44:33:38.8	15.97 B		DA3
HE 2147−1405	21:50:03.69	−13:51:45.9	15.94 B	(PHL 167)	DA2
WD 2151−015	21:54:06.53	−01:17:10.9	14.41	G 093−053,L 1003−016	DA2
HE 2217−0433	22:20:05.80	−04:18:44.5	16.28 B		DA3
WD 2313−330	23:16:02.90	−32:46:41.4	15.74 B	HK 22888−45, MCT	DA1

only the σ^- component is discernible. The Hα components of the first spectrum are split by 1.8 ± 0.3 Å, from which B = 90 ± 15 kG can be derived, a more precise value than the previous estimate.

WD 1953−011. A weak Zeeman-split triplet of Hα was found by Koester et al. (1998), from which they derived a field strength of 93 kG. Maxted et al. (2000) had noticed a variable depression in the wings of Hα which they identified as additional Zeeman-split Hα features, which led them to assume a non-simple field geometry with a strong spot-like field of ∼500 kG combined with a weaker 70 kG dipole field. Comparing the two SPY spectra, the Hα wings appear deformed near 6550 Å and 6575 Å, which might allow a very rough estimate of field strengths of ∼500 kG up to ∼750 kG, if it is assumed that these features are of magnetic origin. However no variation of these features as described by Maxted et al. can be found, the line shape is very similar in both SPY spectra. The central triplet however is obvious, and the splitting of the core is 1.9 ± 0.2 Å. This corresponds to a dipole B field of 95 ± 10 kG.

WD 2105−820. The spectrum of this star was found to show a flat-bottom Hα core, probably due to a low magnetic field, by Koester et al. (1998), from which they derive a field strength of 43 kG. No Zeeman triplet is obvious in the SPY spectra as well, they also only exhibit the broadened, flat core; the full width of the core of 1.8 Å in the SPY spectra is consistent with the field strength derived by Koester et al. (1998).

WD 2359−434. Koester et al. (1998) suspected that this DA could be magnetic due to its flat Hα core, and a very low field

of only 3 kG was polarimetrically found by Aznar Cuardrado et al. (2004). They selected this object as one of their program stars based on the criterion that the SPY spectra show no signs of Zeeman splitting; however they themselves note that flat Balmer line cores are present in the spectra of that object, and if these are caused by the B field, it would indicate a higher field strength than that derived from the polarimetry data. Kawka et al. (2007) measure a low field of 3.4 ± 4.4 kG.

The SPY spectra indeed do not only show a flat-bottom Hα core, but within that core also a pronounced π component and less clear, broad σ components, centered at 6561.1 Å, 6563.5 Å, and 6565.8 Å. Thus a field strength of 110 ± 10 kG can be derived. This is two orders of magnitude stronger than found by Aznar Cuardrado et al. (2004) and Kawka et al. (2007). The reason for these different results is unclear.

WD 0446−789 and WD 1105−048. These objects are the two remaining of the three for which Aznar Cuardrado et al. (2004) discovered magnetic fields of only a few kG from polarimetry data. The Hα core of WD 0446−789 appears slightly broadened, the width is 1.8 Å, which is slightly wider than the average line core width of ∼1 Å. If we interpret this excess width as due to magnetic broadening, this would correspond to a field strength on the order of 10 kG. The line core of WD1105-048 shows no peculiarities, it has a normal width of 1 Å and thus no detectable field.

HS 0051+1145. This object has previously been found as a blue source, PHL 886, but was not observed spectroscopically before the SPY. It is a new magnetic DA. The SPY spectra have a rather low S/N and thus only the Hα triplet of one of the spectra is resolved. The components are placed at 6558.9 Å, 6563.6 Å, and 6568.6 Å, yielding an approximate field strength of 240 ± 10 kG.

HE 1233−0519. This DA was published by Koester et al. (2001), but not recognized as a magnetic star. The SPY spectra have a low S/N such that only the Hα triplet is discernible in one of the spectra. With the components at 6552.2 Å, 6564.4 Å, and 6576.6 Å, a field strength of 610 ± 10 kG results.

WD 2051−208. Beers et al. (1992) published this object as a DA, but it was not further investigated since. It is a new magnetic DA, and shows a variable Zeeman splitting of Hα and Hβ. The Hα components in the two SPY spectra are found at 6562.0 Å, 6566.6 Å, 6570.7 Å, and at 6560.2 Å, 6566.6 Å, 6571.9 Å, respectively, and those of Hβ at 4861.2 Å, 4864.0 Å, 4866.7 Å, and at 4861.0 Å, 4863.9 Å, 4866.9 Å. The resulting field strengths are 220 ± 20 kG and 290 ± 20 kG (from Hα) as well as 250 ± 30 kG and 270 ± 30 kG (from Hβ). The values derived from Hα are significantly different, and each is consistent with the corresponding value from Hβ.

WD 2253−081 and WD 1344+106. Bergeron et al. (2001) suspected that shallow line cores which they found for these objects might indicate low-strength magnetic fields. The line cores of both objects have since been fitted with rotationally broadened line profiles, corresponding to projected rotation velocities of 36^{+14}_{-7} km s^{-1} for WD 2253−081 (Karl et al. 2005) and 4.5 ± 2 km s^{-1} for WD 1344+106 (Berger et al. 2005). The

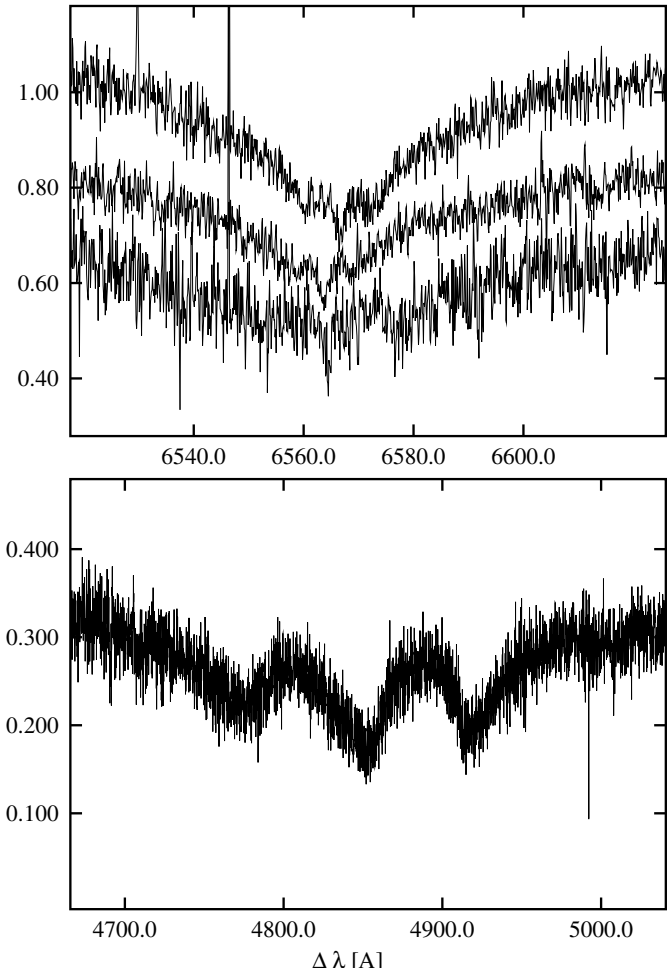

Fig. 5. Four new magnetic DAs. *Top panel*: Hα in WD2051-208, HS0051+1145, HE1223-0519 (from *top*). *Bottom*: Hβ in HS1031+0343. Vertical axis is relative intensity, with arbitrary offsets between spectra for clarity.

Hα line cores in the SPY spectra of both objects neither show Zeeman triplets nor flat bottoms that could indicate the presence of a B field. They are non-magnetic objects.

HS0209+0832. This DAB star is well studied since it is one of very few objects that exhibit helium features at a temperature that places it in the DB gap (Jordan et al. 1993). Heber et al. (1997) found a helium abundance that is variable at timescales of a few months, which has been interpreted as a sign of helium accretion from a clumpy interstellar medium. The equivalent widths of the He I 4471 Å and 5876 Å lines show no significant differences between both SPY spectra, i.e., no variation of the abundance is found. This is however not surprising since the spectra were recorded within 3 days of each other.

Zeeman splitted Hα or Hβ for the four new magnetic DAs are displayed in Fig. 5.

6. Binaries with DA white dwarfs and dM companions

Table 3 gives the data on binaries containing a DA and a M dwarf companion, identified from molecular features in the red spectrum and/or Balmer emission components. The names in boldface indicate new detections from the SPY. The magnitude

is the Johnson V magnitude, unless indicated otherwise (see description for Table 1). The type is estimated from the effective temperature obtained with a fit with hydrogen models, using only the higher Balmer lines from Hγ.

7. Conclusions

We present the data – coordinates, magnitudes, and alias names – for the hydrogen-rich objects in the SPY sample. These include 615 objects with pure hydrogen spectra, for which atmospheric parameters derived from fits with hydrogen models are given in Table 1. Of these, 187 are new white dwarf detections from this survey, or the HES and HQS surveys used to define the target list. In addition to the 615 DAs, our sample also includes 46 DA+dM binaries, of which 10 are new, and 10 magnetic DA (4 new). The results show that with careful reduction even high-resolution echelle spectra can be used to determine stellar parameters through line profile fitting, although the line profiles may extend over many echelle orders. However, there is an indication that the surface gravities obtained are lower by 0.05−0.08 dex, compared to results from high S/N low-resolution spectra. The surface gravities of the normal DAs show the well known, but still unexplained, trend to a larger value (by 0.2 dex) for temperatures below approximately 12 500 K.

Acknowledgements. T.L. is supported within the framework of the Excellence Initiative by the German Research Foundation (DFG) through the Heidelberg Graduate School of Fundamental Physics (grant number GSC 129/1). Research at Bamberg in the context of the SPY project was funded by the DFG through grants Na 365/2-1/2 and He 1356/40-3/4. This research has made extensive use of the SIMBAD database, operated at CDS, Strasbourg, France.

References

Adelman-McCarthy, J. K., Agueros, M. A., Allam, S. S., et al. 2008, ApJS, 175, 297
Aznar Cuardrado, R., Jordan, S., Napiwotzki, R., et al. 2004, A&A, 423, 1081
Beers, T. C., Preston, G. W., Shectman, S. A., Doinidis, S. P., & Griffin, K. E. 1992, AJ, 103, 267
Berger, L., Koester, D., Napiwotzki, R., Reid, I., & Zuckerman, B. 2005, A&A, 444, 565
Bergeron, P. 1992, JRASC, 86, 309
Bergeron, P., Wesemael, F., Fontaine, G., & Liebert, J. 1990a, ApJ, 351, L21
Bergeron, P., Liebert, J., & Greenstein, J. L. 1990b, ApJ, 361, 190
Bergeron, P., Ruiz, M. T., & Leggett, S. K. 1997, ApJS, 108, 339
Bergeron, P., Leggett, S. K., & Ruiz, M. T. 2001, ApJS, 133, 413
Bergeron, P., Fontaine, G., Billéres, M., et al. 2004, ApJ, 600, 404
Brown, W. R., Geller, M. J., Kenyon, S. J., & Kurtz, M. J. 2006, ApJ, 640, L35
Castanheira, B. G., Kepler, S. O., Mullally, F., et al. 2006, A&A, 450, 227
Christlieb, N., Wisotzki, L., Reimers, D., et al. 2001, A&A, 366, 898
Cutri, R. M., Skrutskie, M. F., Van Dyk, S., et al. 2003, CDS/ADC Collection of Electronic Catalogues, 2MASS All Sky Catalog of point sources, 2246, 0
DeGennaro, S., von Hippel, T., Winget, D. E., et al. 2008, AJ, 135, 1
Demers, S., Wesemael, F., Irwin, M. J., et al. 1990, ApJ, 351, 271
Eisenstein, D. J., Liebert, J., Koester, D., et al. 2006, AJ, 132, 676
Gianninas, A., Bergeron, P., & Fontaine, G. 2005, ApJ, 631, 1100
Greenstein, J. L., & Liebert, J. W. 1990, ApJ, 360, 662
Hagen, H.-J., Groote, D., Engels, D., & Reimers, D. 1995, A&AS, 111, 195
Heber, U., Napiwotzki, R., Lemke, M., & Edelmann, H. 1997, A&A, 324, 53
Homeier, D. 2001, Ph.D. Thesis, University of Kiel
Homeier, D., Koester, D., Hagen, H.-J., et al. 1998, A&A, 338, 563
Jordan, S., Heber, U., Engels, D., & Koester, D. 1993, A&A, 273, L27
Karl, C. A., Heber, U., & Napiwotzki, R. 2005, in 14th European Workshop on White Dwarfs, ed. D. Koester, & S. Moehler, ASP Conf. Ser., 334, 369
Kawka, A., & Vennes, S. 2006, ApJ, 643, 402
Kawka, A., Vennes, S., Schmidt, G. D., Wickramasinghe, D. T., & Koch, R. 2007, ApJ, 654, 499
Kepler, S. O., Giovannini, O., Kanaan, A., Wood, M. A., & Claver, C. F. 1995, BaltA, 4, 157
Kepler, S. O., Kleinman, S. J., Nitta, A., et al. 2007, MNRAS, 375, 1315
Kilkenny, D., O'Donogue, D., & Stobie, R. S. 1991, MNRAS, 248, 664
Kleinman, S. J., Harris, H. C., Eisenstein, D. J., et al. 2004, ApJ, 607, 426
Koester, D. 2009, in press in Mem. Soc. Astron. Ital. [arXiv:0903.1499]
Koester, D., Dreizler, S., Weidemann, V., & Allard, N. F. 1998, A&A, 338, 612
Koester, D., Napiwotzki, R., Christlieb, N., et al. 2001, A&A, 378, 556
Koester, D., Rollenhagen, K., Napiwotzki, R., et al. 2005, A&A, 432, 1025
Koester, D., Kepler, S. O., Kleinman, S. J., & Nitta, A. 2009, in Proceedings of the 16th European Workshop on White Dwarfs, Barcelona 2008, in press [arXiv:0812.0491]
Lamontagne, R., Demers, S., Wesemael, F., Fontaine, G., & Irwin, M. J. 2000, AJ, 119, 241
Liebert, J., Bergeron, P., & Holberg, J. B. 2005, ApJS, 156, 47
Lisker, T., Heber, U., Napiwotzki, R., et al. 2005, A&A, 430, 223
Marsh, T. R., Dhillon, V. S., & Duck, S. R. 1995, MNRAS, 275, 828
Maxted, P. F. L., Ferrario, L., Marsh, T. R., & Wickramasinghe, D. T. 2000, MNRAS, 315, 41
McCook, G. P., & Sion, E. M. 1999, ApJS, 121, 1
Morales-Rueda, L., Marsh, T. R., Maxted, P. F. L., et al. 2005, MNRAS, 359, 648
Mukadam, A. S., Mullally, F., Nather, R. E., et al. 2004, ApJ, 607, 982
Napiwotzki, R., Green, P, J., & Saffer, R. A. 1999, ApJ, 517, 399
Napiwotzki, R., Christlieb, N., Drechsel, H., et al. 2001, Astron. Nachr., 322, 411
Napiwotzki, R., Christlieb, N., Drechsel, H., et al. 2003, The Messenger, 112, 25
Napiwotzki, R., Yungelson, L., Nelemans, G., et al. 2004, ASPC, 318, 402
Nelemans, G., Napiwotzki, R., Karl, C., et al. 2005, A&A, 440, 1087
Pauli, E.-M., Napiwotzki, R., Altmann, M., et al. 2003, A&A, 400, 877
Pauli, E.-M., Napiwotzki, R., Heber, U., Altmann, M., & Odenkirchen, M. 2006, A&A, 447, 173
Press, W. H., Teukolsky, S. A., Vetterling, W. T., & Flannery, B. P. 1992, Numerical Recipes, second edition, University of Cambridge, Cambridge
Silvotti, R., Voss, B., Bruni, I., et al. 2005, A&A, 443, 195
Stroeer, A., Heber, U., Lisker, T., et al. 2007, A&A, 462, 269
Voss, B. 2006, Ph.D. Thesis, Universität Kiel
Voss, B., Koester, D., Østensen, R., et al. 2006, A&A, 450, 1061
Voss, B., Koester, D., Napiwotzki, R., Christlieb, N., & Reimers, D. 2007, A&A, 470, 1079
Werner, K., Rauch, T., Napiwotzki, R., et al. 2004, A&A, 424, 657
Wisotzki, L., Koehler, T., Groote, D., & Reimers, D. 1996, A&AS, 115, 227